Cation effects in hydrogen evolution and CO₂-to-CO conversion: A critical perspective

Yu-Shen Hsu, ¹ Sachinthya T. Rathnayake, ¹ and Matthias M. Waegele^{1, a)}
Department of Chemistry, Merkert Chemistry Center, Boston College, Chestnut Hill, Massachusetts 02467,
United States

(Dated: 15 March 2024)

The rates of many electrocatalytic reactions can be strongly affected by the structure and dynamics of the electrochemical double layer (EDL), which in turn can be tuned by the concentration and identity of the supporting electrolyte's cation. The effect of cations on an electrocatalytic process depends on a complex interplay between electrolyte components, electrode material and surface structure, applied electrode potential, and reaction intermediates. Although cation effects remain insufficiently understood, the principal mechanisms underlying cation-dependent reactivity and selectivity are beginning to emerge. In this perspective, we summarize and critically examine recent advances in this area in the context of the hydrogen evolution reaction (HER) and CO₂-to-CO conversion, which are among the most intensively studied and promising electrocatalytic reactions for the sustainable production of commodity chemicals and fuels. Improving the kinetics of the HER in base and enabling energetically efficient and selective CO₂ reduction at low pH are key challenges in electrocatalysis. The physical insights from the recent literature illustrate how cation effects can be utilized to help achieve these goals and to steer other electrocatalytic processes of technological relevance.

I. INTRODUCTION

The development of efficient processes for the interconversion of electrical and chemical energy is central to building a sustainable economy. Electrocatalysts enable these transformations by facilitating the syntheses of renewable fuels and valuable commodity chemicals from abundant and renewable feedstocks in electrolyzers; in fuel cells, they help liberate energy stored in chemical bonds. However, the energy efficiency and product selectivity of many electrocatalytic processes are still too low for them to be practical. 2-4 For example, the rates of the hydrogen evolution reaction (HER) on Pt (and many other catalysts) are up to several orders of magnitude lower in base than in acid,^{5,6} a significant hurdle in alkaline water electrolysis. During the electrolysis of CO₂, the HER is often a competing reaction that lowers the product selectivity for desirable CO₂ reduction products.^{7,8} Further advances in designing electrocatalytic interfaces are needed to make these processes industrially viable.

Electrocatalytic interfaces emerge from bringing an electrode into contact with an electrolyte. Therefore, electrocatalytic activity is not dictated by the electrode alone but is often strongly influenced by the electrolyte composition. The coupling of electrode and electrolyte gives rise to the electrochemical double layer (EDL), a thin layer of electrolyte in the vicinity of the electrode whose chemical and physical properties are distinct from those of the bulk electrolyte. The EDL is the environment in which electrocatalytic processes occur. The careful design of the EDL therefore plays an essential part in enhancing the energy efficiency and product

a) Electronic mail: waegele@bc.edu

selectivity of electrocatalytic interfaces.

To steer electrocatalytic processes, the structure and dynamics of the EDL can be tuned in a variety of ways. An effective strategy of EDL tuning involves the careful choice of the cationic species of the electrolyte, which tend to strongly accumulate at the interface under cathodic polarization. These cationic species can be a minority component that is introduced into the supporting electrolyte. For example, the presence of cetyltrimethylammonium, a cationic surfactant, at a bulk concentration of 67 μ M during CO₂ reduction on Cu at $-0.7 V_{\rm BHE}$ (RHE = reversible hydrogen electrode) decreases the selectivity for the HER from $\sim 85\%$ to $\sim 35\%$ and increases that for CO₂-to-CO conversion from <2% to $\sim 10\%$.¹² The judicious choice of the supporting electrolyte's cation often also has a strong effect on the rates. For example, on SnO₂ electrodes in acid (pH 1) in the absence of metal cations, the rate of CO₂ reduction is insignificant and the HER dominates.⁸ However, in the presence of 0.4 M K⁺ at the same pH, the faradaic efficiencies for formic acid and CO reach $\sim 70\%$ and $\sim 8\%$ at -1.34 V_{RHE}, respectively, indicating that the introduction of K⁺ activates CO_2 reduction and suppresses the HER.

Cation effects are not limited to the HER and CO₂ reduction but are a more general phenomenon. A wide range of electrocatalytic reactions, including the oxygen reduction reaction (ORR), ^{13,14} oxygen evolution reaction (OER), ^{15,16} nitrogen reduction reaction (NRR), ¹⁷ hydrogen peroxide reduction, ¹⁸ and hydrogenation and oxidation of organic molecules ^{19,20} are affected by the choice of the cation. However, steering electrocatalysis by means of cation effects is challenging. The impact of cations on the properties of the electrocatalytic interface not only depends on cation identity and concentration, but is also mediated by many other factors, such as anion identity, pH, electrode structure and material, applied electrode potential, and the relevant intermediates of the reac-

tion.¹⁰ It is this complex interplay that makes it so challenging to understand cation effects and to leverage them to their full extent for facilitating desirable processes.

Observations of the effects of cations on the HER in the 1920s²¹ inspired Frumkin to develop a theoretical framework for understanding these effects. ^{22,23} An expression similar to Frumkin's model was recently derived on the basis of a Marcus-type theory.²⁴ Apart from the Frumkin model, a range of additional hypotheses have emerged to rationalize cation effects. In 2019, we summarized the key ideas and sketched the historic development of this field in a perspective article in this Journal. 10 Since our earlier perspective, research in this area has further intensified and new ideas have been proposed, making it challenging to reconcile the apparent diverse observations and views. Herein, we aim to synthesize a cohesive picture of the principal mechanisms by which alkali cations impact the HER and CO₂-to-CO conversion and identify points of contention.

We purposely restricted this perspective to experimental studies on the effects of alkali cations on the HER and CO₂-to-CO conversion catalyzed on metal electrodes that have been published since our 2019 perspective. The impact of alkali cations on these two reactions has been most intensely studied in the last 2-3 years, allowing us to contrast findings and interpretations as well as to find commonalities between views. We do not examine studies that focus on other reactions or cations, unless the insights derived from the work are directly related to the discussion. Because our expertise lies in experimental investigations, we primarily critique experimental studies and only discuss theoretical work as needed. This article aims to complement recent reviews, ^{25–30} perspectives, 31,32 and accounts 33 on EDL structure and dynamics and its impact on electrocatalysis.

This article is structured as follows: In section II A we review key results regarding the effects of alkali cations on the HER. This section summarizes the findings and interpretations of the respective authors of the articles. In section II B, we then critically examine the findings and provide our perspective. In section III A we summarize key observations on how alkali cations influence CO₂-to-CO conversion. In section III B, we then provide our critical assessment by first describing the accumulation and distribution of cations in the EDL (section III B 1) and then discussing possible mechanisms of CO₂ promotion (section III B 2). In section IV, we provide an outlook.

II. HYDROGEN EVOLUTION REACTION

A. Key Results

In this section, we summarize several representative studies on how cations affect the HER. The studies primarily focus on the HER in alkaline media, that is, the conclusions drawn are applicable to the reduction of water (and not to the reduction of hydronium ions, which is typically

mildly to moderately impeded by alkali cations^{8,34}). For each study, we give the key observations and the interpretation provided by the authors and describe the experimental and computational evidence for it. In the next section, we collectively view the findings reported in these studies and provide our assessment.

The studies of Goyal et~al.³⁷ and Monteiro et~al.³⁵ established that alkali cations can promote or inhibit the HER on Au and Pt in base, depending on the degree of cation accumulation, which is tuned by electrode material and electrolyte pH for a fixed RHE potential. They showed that alkali cations promote the HER under alkaline conditions on Au at low overpotentials, but inhibit the reaction at more cathodic potentials (Fig. 1A). The crossover potential separating the promotion from the inhibition regime shifts to more positive RHE potentials with increasing pH, indicating that the degree of cation accumulation in the EDL is tuned by the pH for a given RHE potential. The authors suggested that the promotion arises from acceleration of the Volmer step by alkali cations stabilizing the transition state of the dissociating water molecule.³⁷ At more cathodic potentials, they concluded that larger cations strongly accumulate in the outer Helmholtz plane (OHP) to a degree that interferes with access of water to surface sites. They proposed that the accumulation of cations with smaller crystal radii (for example, Li⁺) is limited by their tightly bound hydration shells. Monteiro et al. argued that, in contrast to Au, Pt is mostly in the inhibition regime because it interacts with cations with larger crystal radius more strongly than Au.³⁵

On Au, Monteiro et al. observed Tafel slopes of ≈ 120 mV/dec, suggesting that the Volmer step is the ratedetermining step (RDS), irrespective of pH and type of electrolyte cation.³⁵ At low overpotentials and pH 11, the reaction order in K^+ (≈ 0.8) is larger than the one in Li^+ (≈ 0.3) , confirming that K⁺ promotes the Volmer step more than Li⁺ under these conditions. Interestingly, at pH 13 the reaction order in K⁺ is negative, consistent with the notion that accumulation of K⁺ above a certain threshold is detrimental to the kinetics of the Volmer step. The potential and pH at which this threshold is reached is also determined by the metal of the electrode. On Pt, there is a change in the Tafel slope from 43 to 112 mV/dec when going from Li⁺- to K⁺-containing electrolyte at pH 13. This change is consistent with a switch in the RDS from the Heyrovsky to the Volmer step. This observation therefore suggests that K⁺ interferes with hydrogen adsorption by hindering access of water to the surface. The transition from the promotion to the inhibition regime for the HER on Pt can be clearly observed by the change in reaction order in K⁺ at pH 10 (Fig. 1B).

This study also explored to what extent the cations influence the stability of surface-adsorbed hydroxide (OH $_{\rm ads}$), which has been hypothesized to play a key role in water dissociation on Pt. $^{6,38-40}$ The authors concluded that destabilization of OH $_{\rm ads}$ by cations cannot be the sole reason for the observed cation-dependent activity: In

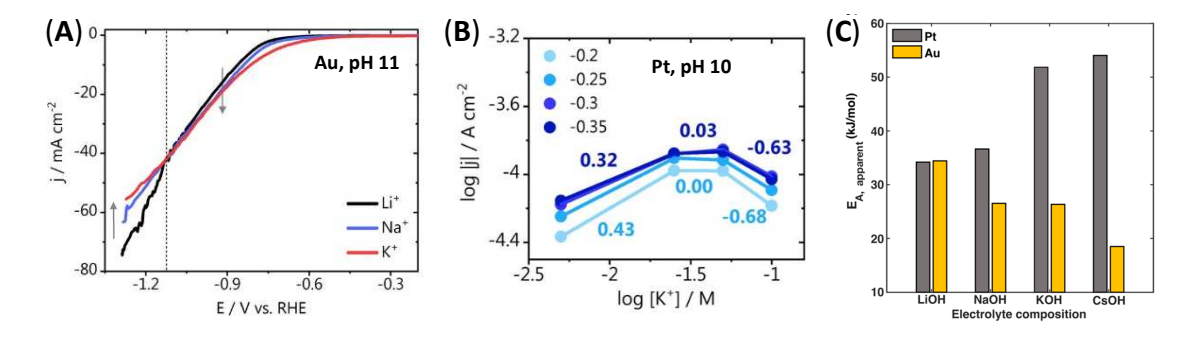


FIG. 1. Electrokinetics of the HER on Pt and Au. (A) Polarization curve of polycrystalline Au in solutions of the hydroxide salts of alkali metal cations as indicated (pH 11). The dashed vertical line indicates the crossover potential separating the promotion from the inhibition regime. (B) Logarithmic current density plotted versus logarithmic K^+ concentration (pH 10, the K^+ concentration was varied by addition of the corresponding perchlorate salt). Panels A-B reprinted with permission from Monteiro et al. [35]. Copyright (2021) The Authors, Published by the American Chemical Society. (C) Dependence of the apparent activation barrier of the HER ($E_{A, apparent}$) on cation identity for Pt (grey) and Au (yellow). Reprinted with permission from Bender et al. [36]. Copyright (2022) American Chemical Society.

both alkaline and acidic solutions the peak for hydrogen underpotential deposition $(H_{\rm upd})$ shifts positively when going from Li⁺ to K⁺ (albeit to different extents), but the effect of the cations on the HER is opposite in the acidic and alkaline regimes.

In another study, Monteiro et al. examined the effects of mono-, di-, and tri-valent cations on the competition between the HER and CO₂-to-CO conversion on Au electrodes in electrolytes at pH 3.³⁴ They found that the cations do not significantly affect H₃O⁺ reduction on Au. By contrast, the potential at which H₂O reduction steeply increases is shifted anodically with increasing charge on the cation from monovalent (Cs⁺, Li⁺) to divalent (Ba²⁺, Be²⁺, Ca²⁺, Mg²⁺) to trivalent (Al³⁺, Ce³⁺, Nd³⁺), but the degree of the activity enhancement varies greatly within a valence group. Within a group, the more weakly hydrated cations (Cs⁺, Ba²⁺, Ce³⁺/Nd³⁺) tend to give rise to the highest activity enhancement (with Be²⁺ being an exception because of its high charge density).

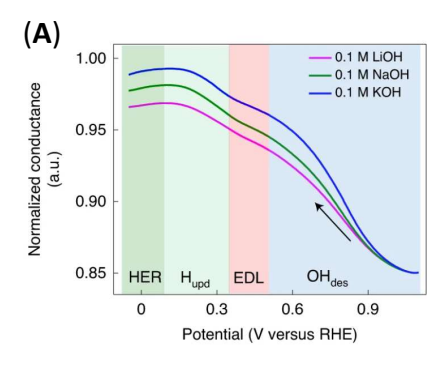
On the basis of *ab initio* molecular dynamics (AIMD) simulations, Monteiro *et al.* explained these trends as the net result of two competing factors:³⁴ First, weakly hydrated cations (of a given valence) have a higher tendency of accumulating in the OHP. The soft hydration shells of these cations facilitate partial desolvation, permitting a higher degree of accumulation in the OHP. Second, the activation barrier of water dissociation decreases with increasing acidity of the cation, the square of the cation's charge divided by its crystal radius. However, with increasing cation acidity the hydration shell becomes harder, thereby limiting the accumulation of the cations in the OHP due to steric repulsion.

Bender et al. measured the dependence of the rate of the HER on alkali-cation identity across reactive metals (Ir, Pd, Pt) and coinage metals (Cu, Ag, Au) in acidic and alkaline media.³⁶ Whereas the rate of the HER is insensitive to the identity of the alkali metal cation at pH 1, it exhibits a pronounced dependence at pH 13. The

HER rate exhibits opposite trends with cation crystal radius, depending on the reactivity of the metal. The cation crystal radius increases from Li⁺ to Cs⁺.⁴¹ For the reactive metals (Ir, Pd, Pt), the HER rate decreases when going from Li⁺ to Cs⁺, whereas the opposite is the case for the coinage metals (Cu, Ag, Au). In the investigated potential regimes, no crossover between promotion/inhibition occurs. Bender et al. explained these observations with the following model: The alkali metal cations primarily influence the rate of the HER by stabilizing the transition state of water dissociation and the resultant interfacial OH⁻ (assumed to not be adsorbed on the electrode). For the coinage metals, stabilization of interfacial OH⁻ promotes the HER. However, for the reactive metals, the additional stabilization lowers the Gibbs free energy of interfacial OH⁻ to an extent that is detrimental to the overall rate. The stabilization could be brought about by electric field or non-covalent cation-hydroxide interactions. This picture explains the observed cation trends across different metals and pH regimes.

Consistent with the proposed picture, the apparent activation barrier derived from Arrhenius analysis of the exchange current decreases on Au with increasing cation crystal radius, whereas the opposite trend holds for Pt (Fig. 1C). On the basis of AIMD simulations and electrochemical experiments with mixtures of cations, Bender *et al.* suggested that the larger the cation crystal radius, the higher the cation's degree of accumulation in the electrochemical double layer. As a result, Cs⁺ accumulates to a higher degree than Li⁺, explaining the distinct impact of the cations on the HER.

Shah et al. measured changes in the surface coverage of OH_{ads} on Pt with electrical transport spectroscopy (ETS) as the potential approaches the HER regime. ETS is thought to exclusively probe surface adsorbates and is insensitive to the interfacial electrostatics and electrode potential. They suggested that OH_{ads} acts as a proton donor and acceptor in the Volmer step. Its avail-



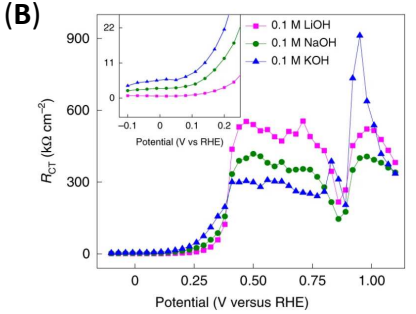


FIG. 2. Cation-Dependent Hydroxide Desorption from Pt and Charge-Transfer Resistance. (A) ETS measurements illustrating the change in normalized conductance with potential in the different alkali metal hydroxides as indicated. The changes are attributable to different degrees of hydroxide desorption. The hydroxide desorption (OH_{des}), EDL, H_{upd} , and HER regions are indicated. (B) Charge-transfer resistance (R_{CT}) as a function of electrode potential. Reprinted with permission from Shah $et\ al.\ [42]$. Copyright (2022) Springer Nature Limited.

ability at the surface is therefore essential for the promotion of this step. The authors suggested that OH_{ads} is destabilized by electrostatic cation- OH_{ads} interactions when going from Li^+ to K^+ , thereby decreasing the availability of OH_{ads} .

ETS indicates that at potentials $>\approx 1 V_{RHE}$ and pH 13, the Pt surface is saturated with OH_{ads}. With decreasing potential, the degree of OH_{ads} desorption depends on the identity of the cation and increases in the order Li⁺. Na⁺. and K⁺ (Fig. 2A). This trend is explained by density functional theory (DFT) calculations and AIMD simulations which show that OH_{ads} is increasingly destabilized by predominantly electrostatic cation- OH_{ads} interactions with larger cation crystal radius. Further experimental evidence for electrostatic cation- OH_{ads} interactions comes from double-layer capacitance measurements. At a potential of ≈ 0.1 V_{RHE}, the capacitance of the interface increases in the order K⁺, Na⁺, and Li⁺. Shah et al. suggested that, in the vicinity of this potential, the capacitance is dictated by the amount of cation accumulation, which in turn depends on the residual population of OH_{ads} . Residual OH_{ads} form anchor points for alkali cations, leading to a higher accumulation of interfacial Li⁺ relative to the other cations at the same bulk concentration. By contrast, at 0.85 V_{RHE} , where the surface is fully hydroxylated, the capacitance increases in the order Li⁺, Na⁺, and K⁺. Here, the cation-surface distance dictates the capacitance. Weakly hydrated cations approach the surface more closely than strongly hydrated Li⁺, giving rise to the reversal of the capacitance trend.

The charge-transfer resistance of the interface mirrors the trends in the interfacial capacitance. The chargetransfer resistance in the potential range where predominately OH_{ads} desorption occurs (0.9 to 0.4 V_{RHE}) is lowest in the presence of K⁺, which destabilizes OH_{ads} relative to Li⁺ and Na⁺ (Fig. 2B). By contrast, in the H_{upd} region, Li⁺ gives rise to the lowest charge-transfer resistance, suggesting that it facilitates the Volmer step. The authors proposed that the mechanism of Volmer step promotion is not due to the activation of water in the hydration shell of alkali cations. Indeed, their DFT calculations suggest a strengthening of the O-H bond of water in the hydration shells of the cations. Rather, the DFT and AIMD calculations show that $\mathrm{OH}_{\mathrm{ads}}$ can act as a proton donor and acceptor in the Volmer step, thereby increasing the rate of the HER.

Huang et al. explored the impact of cation identity on the structural and dielectric properties of interfacial water on a Pt electrode during the HER and the hydrogen oxidation reaction (HOR) in 0.1 M alkali hydroxides. ⁴³ They found that the higher degree of cation accumulation with increasing crystal radius of the cation weakens the H-bonding network of interfacial water and increases the static dielectric constant. The cation-induced structural change of the solvation structure of the interface manifests itself in a higher reorganization energy and a smaller reaction entropy for the HER with increasing cation crystal radius. Therefore, they attributed the cation-dependent HER/HOR rates to cation-induced changes in the solvation structure of the electrocatalytic interface.

Huang et al. demonstrated that the reorganization energy (from application of the Marcus-Hush-Chidsey (MHC) model) and the activation barrier (from Arrhenius analysis) increase with increasing cation crystal radius.⁴³ The reaction entropy, derived from the temperature-dependence of the formal potential of the HER/HOR, decreases when going from Li⁺ to Cs⁺. Huang et al. proposed that the enthalpic contribution to the Gibbs free energy of reaction of the HER is rather small, as measured by the minute effect of the identity of alkali cations on the hydrogen desorption/hydroxide adsorption peaks in the CV of a Pt electrode. They concluded that the entropic contribution is much larger than the enthalpic contribution to the Gibbs free energy of reaction. With decreasing reaction entropy, the exchange current density decreases and the reorganization energy increases (Fig. 3A). To gain insights into the origin of the altered energetics, Huang et al. probed changes in the structure of interfacial water as a function of cation identity with surface-enhanced infrared absorption spectroscopy (SEIRAS). A high-frequency shoulder at ≈ 3570

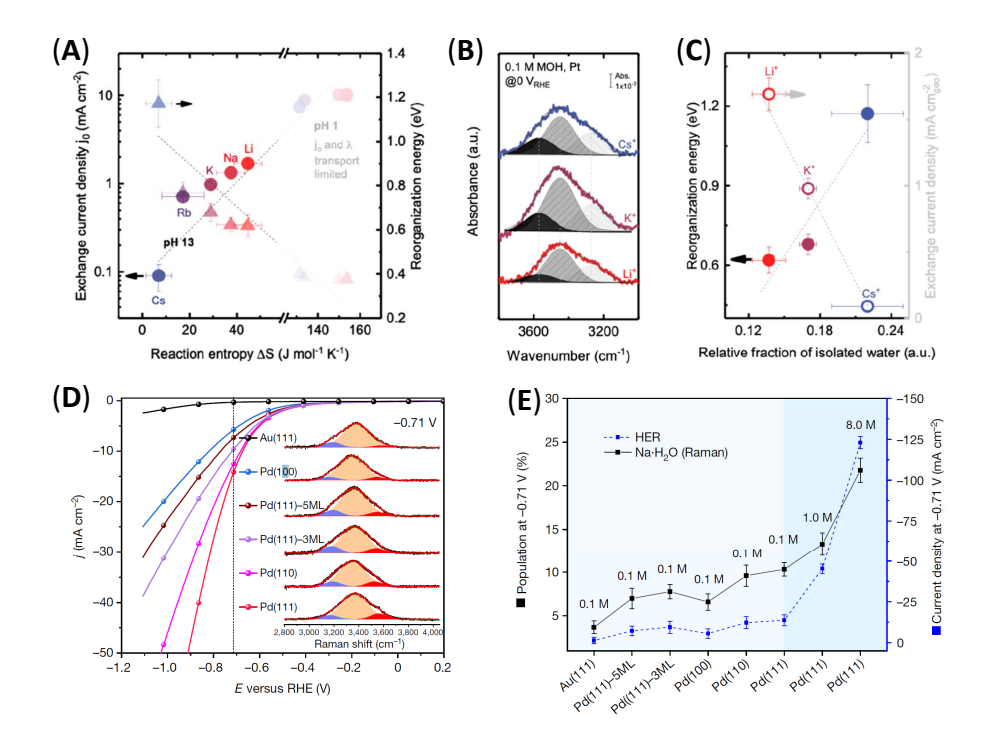


FIG. 3. Correlation of Water Structure and Reaction Entropy with HER Kinetics. (A) Exchange current density (left axis) and reorganization energy (right axis) for the HER on Pt as a function of reaction entropy. The reorganization energy was determined from application of the MHC formalism to experimental data. The reaction entropy (abscissa) was derived from the temperature-dependence of the formal potential of the HER/HOR. Electrolytes: Alkali metal hydroxides (pH 13) and perchlorates (pH 1). (B) SEIRA spectra of the O-H stretch of water at the Pt/electrolyte interface in the presence of 0.1 M of the hydroxide salts of the alkali metal cations as indicated. The black band corresponds to weakly H-bonded (isolated) water molecules. (C) Reorganization energy (left axis) and exchange current density (right axis) as a function of the fraction of isolated water relative to other types of interfacial water. Panels A-C reprinted with permission from Huang et al. [43]. Copyright (2021) The Authors, Published by the American Chemical Society. (D) HER current density on different electrodes as indicated. The inset shows SHINER spectra of the O-H stretch of interfacial water with the band of weakly H-bonded water indicated in red. Electrolyte: 0.1 M NaClO₄ (pH 11). (E) Population of weakly hydrogen-bonded water (left axis) and HER current density (right axis) for Au(111) and different crystallographic facets of Pd at an electrode potential of -0.71 V_{RHE}. The concentrations of the electrolyte (NaClO₄) are indicated. Pd(111)-5ML and Pd(111)-3ML denote epitaxially grown 5- and 3-monolayer-thin films on Au(111), respectively. Panels (D) and (E) reprinted with permission from Wang et al. [44]. Copyright (2021) Springer Nature Limited.

cm⁻¹ develops in the OH-stretching band of interfacial water when going from Li⁺ to Cs⁺ (Fig. 3B). This band is attributable to weakly H-bonded/isolated waters. The reorganization energy correlates with the population of isolated waters (Fig. 3C). On the basis of these observations, Huang *et al.* proposed that the barrier for the HER is predominately entropic and that strongly hydrogenbonded water facilitates the reorganization of the interfacial solvation structure during the reaction.

Wang et al. probed the HER on Pd single-crystal electrodes as a function of $NaClO_4$ concentration at pH 11.⁴⁴ They proposed that H_2O molecules in the hydration shell of Na^+ can approach the Pd electrode surface more closely than other types of interfacial water and exhibit a higher probability of pointing their H-atoms towards the surface. Because the closer distance facilitates electron transfer from the electrode to water and the preferential orientation primes the water for H^+ -transfer, they

suggested that this water is more easily dissociated.

They observed that with decreasing potential and increasing Na⁺ concentration, the population of weakly hydrogen bonded water (with a band at $\approx 3540 \text{ cm}^{-1}$) increases as assessed with shell-isolated nanoparticleenhanced Raman spectroscopy (SHINERS). They attributed this band to H₂O in the hydration shell of Na⁺. The enrichment of this species coincides with an increase in the amplitude of the librational band and a red-shift of the H₂O bending mode. When taken together, these data indicate a weakening of the H-bonding network with decreasing electrode potential. They observed that the HER activity on different crystal facets of Pd tracks the population of weakly H-bonded interfacial water on these surfaces (Fig. 3D and E). The $\approx 3540 \text{ cm}^{-1}$ band also exhibits a larger Stark tuning slope, suggesting that the water molecules in the hydration shell of Na⁺ are preferentially aligned with the interfacial electric field. Their

AIMD calculations predict that these water molecules can approach the Pd electrode more closely than water in other H-bonding configurations and more readily accept an electron from the electrode, thereby facilitating the Volmer step.

Ding et al. hypothesized that the rate of the HER (and those of other electrocatalytic reactions) is dependent on the ability of the solvent structure in the EDL to reorganize itself following interfacial charge transfer. 14,45 The interfacial water dipoles most easily re-orientate themselves following a disturbance (such as interfacial charge transfer) at the potential of maximum entropy (PME). At electrode potentials significantly away from the PME, an interfacial electric field exists that imposes a net orientation on the water dipoles, rendering their reorganization more difficult. On the basis of this reasoning, the rate of the HER is expected to increase as the PME moves towards the thermodynamic equilibrium potential of the reaction. Using laser-induced current transients, Ding et al. measured the PME of Pt and Au electrodes in the presence of different alkali cations. Indeed, consistent with their hypothesis, they observed that the PME on polycrystalline Pt shifts from ${\sim}0.11$ to ${\sim}0.25$ V_{RHE} when going from Li^+ to Cs^+ (at pH 6 and SO_4^{2-} as the counterion), as shown in Fig. 4A. Although these shifts are rather small, Ding et al. observed a large shift of $\sim 0.92 \text{ V}$ in the PME of polycrystalline Au when switching the electrolyte from 0.5 M Na₂SO₄ to K₂SO₄ (pH $6).^{45}$

Using phase-sensitive second-harmonic generation (PS-SHG). Xu et al. determined the second-order and third-order nonlinear susceptibilities of the Pt/alkaline electrolyte interface in the presence of K⁺, Li⁺, and Ba²⁺ (Fig. 4B).⁴⁶ The second-order susceptibility $(\chi_{\rm s}^{(2)})$ is influenced by the centrosymmetry of the hydration shells of the cations at the interface. The higher $\chi_{\rm s}^{(2)}$ in the presence of K⁺ compared with that in Li⁺- and Ba²⁺containing electrolyte suggests that the hydration shell of interfacial K⁺ has a lower centrosymmetry compared with those of the more strongly hydrated cations. Xu et al. suggested that the interfacial polarization deforms the hydration shell of the more weakly hydrated K⁺ to a larger extent. The third-order susceptibility $(\chi_s^{(3)})$ is influenced by the degree to which the interfacial electric field imposes a net orientation on interfacial water (predominantly on water outside the hydration shells of ions). The smaller $\chi_s^{(3)}$ in Li⁺- and Ba²⁺-containing electrolyte suggests that their presence hinders the alignment of interfacial water with the EDL field. Xu et al. suggested a cation-mediated HER mechanism reminiscent of the model proposed by Bender et al.,36 as described earlier in this section.

Cations have also been proposed to indirectly modulate the HER by interactions with anions. For example, Jackson *et al.* demonstrated that phosphate ions can act as proton donors during the HER on Au electrodes in phosphate buffer at neutral pH, thereby greatly promot-

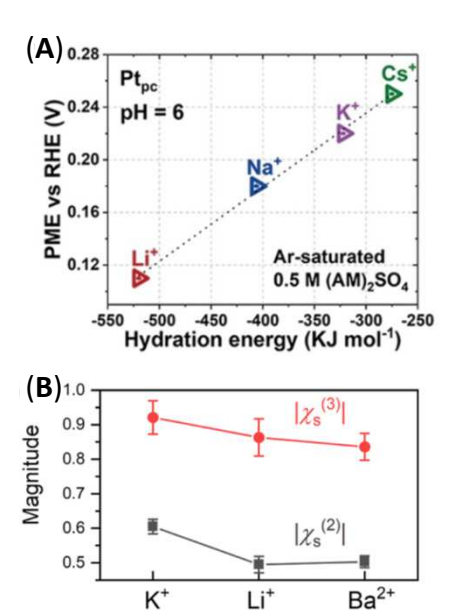


FIG. 4. Dependence of Orientation of Interfacial Water on Cation Identity. (A) PME of a polycrystalline Pt electrode in 0.5 M (AM)₂SO₄ at pH 6 (AM = alkali metal). Reprinted with permission from Ding et al. [14]. Copyright (2021) The Authors, Published by Wiley-VCH GmbH.(B) Dependence of the second-order ($\chi_s^{(2)}$) and third-order ($\chi_s^{(3)}$) optical susceptibilities of the Pt/electrolyte contact on cation identity. The electrolyte compositions were 0.1 M KOH (K⁺), 0.1 M LiOH (Li⁺), and 0.1 M KOH with 0.1 mM Ba(OH)₂ (Ba⁺). Reprinted with permission from Xu et al. [46]. Copyright (2024) American Chemical Society.

ing the reaction. 47 Jackson $et\ al.$ suggested that cationanion interactions may help pre-organize phosphate prior to proton-coupled electron transfer. Cations can also induce a switch in the proton donor. Studying the HER in ${\rm CO}_2$ -saturated bicarbonate buffer with a rotating ring disk electrode, Marcandalli $et\ al.$ proposed a change in proton donor from water to ${\rm HCO}_3^-$ when the concentration of ${\rm Na}^+$ increases from 0.1 to 0.5 M. 48

B. Critical Assessment

Informed by the collective evidence described in the prior section, we now express our perspective. Each of the studies described therein presented a well-reasoned, cohesive interpretation of the respective observations. Almost all studies agree that cations modulate the energetics of the Volmer or Heyrovsky step, thereby bringing about the cation-dependent HER rates. However, the views diverge in regards to the mechanistic origin of the modulation. The different mechanisms are illustrated in Fig. 5.

We first discuss the hypotheses that focus on interactions of cations with adsorbed/interfacial hydroxide (Fig. 5A). Shah *et al.* presented strong experimental ev-

idence that OH_{ads} on Pt is destabilized when going from smaller to larger cation crystal radius. This evidence includes cation-induced changes in the following quantities: the H_{upd}/OH_{ads} exchange peak in the CV of Pt, surface conductivity, double layer capacitance, and chargetransfer resistance. 42 This interpretation is further bolstered by DFT and AIMD calculations of OH_{ads} that predict a destabilization with increasing cation crystal radius. ^{38,42} However, the role of OH_{ads} in the HER is ascertained to a relatively lesser degree. Shah et al.'s DFT and AIMD calculations suggest that ${\rm OH_{ads}}$ could act as a proton donor/acceptor during the HER. ⁴² By contrast, Huang et al. argued that the impact of alkali cations on the $H_{\rm upd}/OH_{\rm ads}$ exchange peak was too small to account for the observed cation-induced changes in the exchange current of two orders of magnitude. 43 Monteiro et al. observed that the H_{upd}/OH_{ads} exchange peak in the CV of Pt shifts in the same direction when going from Li⁺ to K⁺, in both acidic and alkaline electrolytes, whereas the effect of cation identity on reactivity is opposite in acidic and basic media.³⁵ However, the H_{upd}/OH_{ads} exchange peak may not be a reliable predictor for HER activity. Dubouis et al. noted that the H_{upd} peak on Pt(111)does not change with pH on the RHE scale, whereas the HER activity of Pt(111) decreases by 2-3 orders of magnitude when going from pH 0 to 13.6 On the basis of this and other observations, they argued that H_{upd} is distinct from the reactive hydrogen that participates in the HER.

The discussion in the preceding paragraph illustrates the experimental challenges associated with assessing how cations mediate the role of OH_{ads} in the HER. It would be desirable to conduct this evaluation at more negative potentials ($<-0.1 V_{RHE}$) where cation effects are clearly observed but the surface concentration of OH_{ads} is expected to be small (the potential of zero free charge of polycrystalline Pt is $\sim 0.23 \text{ V}_{\text{SHE}},^{49}$ which corresponds to $\sim 1.0 \text{ V}_{\text{RHE}}$ at pH 13). Using electrokinetic experiments in conjunction with microkinetic modelling, Rebollar et al. concluded that OH_{ads} is not directly involved in the HER mechanism.³⁹ Li et al. suggested that OH_{ads} modulates the interfacial hydrogen-bonding network, thereby influencing HER kinetics.⁵⁰ Taken together, we estimate that cation-induced OH_{ads} destabilization contributes to the observed changes in HER rates, but it is probably not the dominant factor, especially at more cathodic potentials.

The proposal by Bender et al. that alkali cations alter the energetics of water dissociation by stabilizing interfacial hydroxide (not necessarily adsorbed) that forms during the reaction is appealing because it elegantly explains the distinct cation effects across different metals.³⁶ However, the effect of cations on interfacial hydroxide needs to be further explored. As discussed in the prior paragraph, there is strong experimental (and theoretical) evidence that OH_{ads} is destabilized with increasing cation crystal radius on Pt. Further, Huang et al. estimated the activity coefficient of interfacial hydroxide at a Pt electrode.⁴³ Using the dielectric constants of the

interface and the effective radii of OH $^-$ (derived from application of the Born model to their experimental data) and the Davies equation, they found that the activity coefficient of interfacial hydroxide changes from 0.21 to 0.48 when going from Li $^+$ to Cs $^+$. The corresponding change in the Gibbs free energy $(-RT\ln\gamma_{\rm OH}{}^-)$ is -0.038 eV and -0.018 eV for Li $^+$ and Cs $^+$, respectively. Therefore, within the limits of the models, the Gibbs free energy increases with increasing cation crystal radius and the changes are rather small. Although it is possible that interfacial hydroxide is more strongly stabilized by cations with larger crystal radius under certain conditions, further experiments and computations are needed to explore this possibility.

Having examined the theories that focus on the role of adsorbed/interfacial hydroxide (Fig. 5A), we now consider alternative hypotheses regarding the stabilization of the transition state of water dissociation. We distinguish between interpretations that focus on local interactions between cations and water and those that postulate that the stabilization comes about from the influence of the cations on the collective behavior of interfacial water. Although local and collective effects are intertwined, making this distinction is helpful for the following discussion. We start with a local picture. Goyal et al.³⁷ and Monteiro et al. 34,35 proposed that cations directly interact with the activated complex of the dissociating water molecule (Fig. 5B). This picture is mostly based on computational models. However, the observation that the potential at which the activity for water reduction increases steeply shifts more anodically with the valence of the cation can be intuitively interpreted within this picture.³⁴ Further, it has been experimentally demonstrated that water coordinated to alkali cations is more readily reduced than free water (at least in organic media).⁵¹ H nuclear magnetic resonance (¹H NMR) spectroscopy shows a lower electron density around protons in water molecules coordinated to alkali cations (Li⁺, Na⁺) than in the water in (butyl)₄N⁺-containing electrolyte.⁵¹ Taken together, we conclude that the strength of the direct interaction of cations with the activated complex of water dissociation is likely a substantial factor influencing the rate of the HER.

On the basis of the Stark tuning slopes of the O–H stretch of water in the hydration shell of Na⁺, Wang et al. showed that these water molecules preferentially adopt a position and orientation relative to the electrode surface that primes these water molecules for reduction (Fig. 5C).⁴⁴ The spectroscopy of Wang et al. also demonstrates that the accumulation of Na⁺ at the interface induces a change in the collective behavior of interfacial water, as measured by the growth of the librational band (The librational band of water arises from the hindered rotation of the molecules in the condensed phase).⁵² The collective behavior determines the ease with which the interfacial water structure can adjust itself upon charge transfer and is therefore expected to play an important role in the HER. This mechanism is illustrated in Fig. 5D.

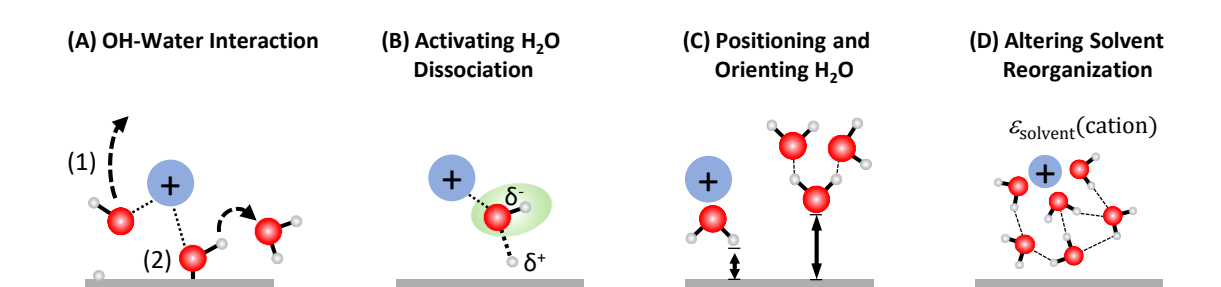


FIG. 5. Cartoon Representations of Proposed Effects of Cations on the HER. (A) Cation (blue filled circle) interacting with interfacial and adsorbed OH^- , represented by white (hydrogen) and red (oxygen) spheres. The cation may influence the removal of interfacial OH^- from the EDL after water dissociation (labeled (1) in the cartoon) or affect the population of adsorbed OH^- (labeled (2) in the cartoon), which may directly (as shown) or indirectly influence the HER. (B) Activation of water dissociation by direct cation/water interactions. (C) Modulation of the orientation and distance between interfacial water and electrode surface by cations. (D) Alteration of the collective structure and dynamics of interfacial water. $\varepsilon_{\text{solvent}}$ represents the dielectric constant of interfacial water, which is cation-dependent.

Cation-induced changes in the collective behavior of interfacial water are manifest in the data of Huang et al., 43,53 Ding et al., 14,45 and Xu et al. 46 However, apparently different mechanisms by which cations alter the water structure and dynamics have been pro-First, Huang et al. found a strengthening of the hydrogen-bonding network of interfacial water with decreasing cation crystal radius. The stronger the hydrogen-bonding network, the lower the reorganization energy of the HER, indicating that a stronger hydrogenbonding network more readily re-organizes itself upon interfacial charge-transfer. Second, Xu et al.'s data indicate that the cation-mediated modulation of the waterwater and water-ion interactions influence the extent to which interfacial water adopts a net orientation in the EDL field, under the assumption that the potential of zero free charge of the electrode is largely invariant in the studied electrolytes. Third, Ding et al. suggested that the net orientation of interfacial water at a given applied electrode potential is primarily dictated by the PME, which they found can significantly shift with cation identity. The PME is closely related to the potential of zero free charge. Taken together, these experiments suggest that the collective behavior of interfacial water is influenced by the concentration and identity of the cation. Further studies are needed to understand the relative weight of these mechanisms under a given set of conditions.

The relationships between exchange current, reorganization energy, and reaction entropy observed by Huang et al. are very interesting but their molecular-level interpretation remains challenging. For example, the extracted reorganization energy includes inner and outer reorganization and therefore does not exclusively reflect solvent reorganization. Nevertheless, the data strongly suggest that the collective behavior of interfacial water plays an important part in facilitating water dissociation. However, only a narrow set of experimental conditions have been explored to date. Further studies with a broader range of catalysts and electrochemical conditions are re-

quired to affirm this interpretation. For example, an open question is to what extent the proposed mechanism by Huang et al. is applicable to catalysts other than Pt. We might expect similar trends in EDL properties (interfacial water structure/dielectric constant) across the series of alkali cations at other electrodes, such as Au. If our notion is correct, the opposite HER activity trends of Pt and Au with increasing crystal radius of the cation would be difficult to explain with this model alone.

The apparently diverging activity trends on Pt and Au may indicate distinct mechanistic regimes as proposed by Goyal $et\ al.^{37}$ and Monteiro $et\ al.^{35}$ a promotion and an inhibition window. The inhibition regime requires further characterization. "Cation overcrowding" has been discussed in more detail in the context of the oxygen evolution reaction 16 and CO_2 reduction 54 .

How cation-induced changes in the hydrogen-bonding network of interfacial water affect the HER requires further study. Wang et al. 44 and Huang et al. 43 found a weakening of the hydrogen-bonding network with increasing cation concentration or cation crystal radius. However, they came to different conclusions regarding how the altered water structure impacts HER. Wang et al. showed that the population of weakly H-bonded water across different facets of Pd semi-quantitatively tracks with the HER rate at a fixed electrode potential. Huang et al. determined that the population of weakly hydrogen bonded/isolated water increases when going from Li⁺ to Cs⁺. Interestingly, they found that the exchange current density decreases with increasing population of weakly Hbonded water, counter to the reactivity trend observed by Wang et al. for HER on Pd in Na⁺-containing electrolyte. Although the results of the two studies cannot be directly compared (as different electrolytes and electrodes were used), the diverging reactivity trends with weakening H-bonding network highlights that further research is needed to understand the impact of interfacial water structure on reactivity.

The preceding discussion shows that an agreement on the principal mechanisms by which cations promote the

Volmer/Heyrovsky steps has yet to emerge. At the heart of this issue lies the fact that a composition change in the EDL impacts a number of interrelated properties of the EDL, including water structure, dielectric constant, and double layer field. It is therefore expected – and often found – that these properties correlate with HER activity, but such correlation does not necessarily identify them as the principal origin of the promotion/inhibition. A way to address this issue might be through physics-based models and advanced computer simulations of the inter $face^{16,55-59}$ that allow one to systematically assess the impact of various EDL properties on reaction steps of interest. Recent experimental studies have quantified EDL properties, such as interfacial electric field, 60-62 dielectic constant, ^{63,64} capacitance, ^{60,65} ion distribution, ^{66,67} or water structure. ^{43,44,46} Such studies are of great importance as the results can be used to benchmark models of the EDL.

It would also be important to extend the understanding to practical reaction conditions. For example, alkaline electrolyzers typically operate at temperatures of ${\sim}80$ °C and electrolyte concentrations of ${\sim}8$ M of KOH. 68 The EDL properties are expected to be substantially different from the experimental conditions used in most analytical studies.

When viewed collectively, the balance of evidence suggests to us that cations impact water reduction in a multifaceted way. Regarding the promotion of the HER, we favor a model in which both the local cation-water interactions (Fig. 5B) as well as the collective response of the interfacial water network (Fig. 5D) play dominant roles. There also appears to be an inhibition regime that probably arises from site-blocking effects. Further research is required to understand how cations can mediate the approach, orientation, and surface excess concentration of anions, especially those that can act as proton donors/acceptors. Using secondary ion mass spectrometry, Zhang et al. found evidence of compact Na⁺/phosphate ion pairs on positively polarized Au electrodes, ⁶⁶ highlighting the complex interplay between electrolyte components.

III. CO2 REDUCTION ON GOLD AND SILVER

A. Key Results

The adsorption of CO_2 on the electrode is commonly accepted as the rate-determining step of CO_2 -to-CO conversion. ^{55,69} Accordingly, stabilization of the resulting $^*\mathrm{CO}_2^-$ intermediate and/or the transition state leading to this intermediate promotes the reaction. With this picture in mind, we summarize several representative studies on cation effects in CO_2 -to-CO conversion.

Monteiro *et al.* investigated CO₂-to-CO conversion on Au, Ag, and Cu electrodes with cyclic voltammetry and scanning electrochemical microscopy in dilute H₂SO₄ solutions (pH 3) with and without alkali cations.⁷⁰ They

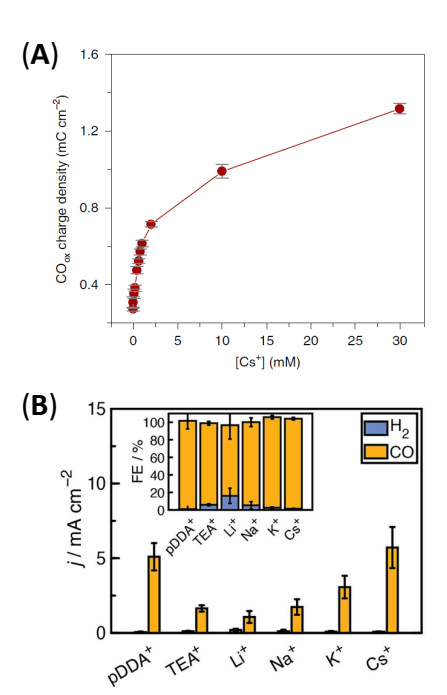


FIG. 6. Effect of Cation Identity on CO₂-to-CO Conversion. (A) Activity of a polycrystalline Au electrode immersed in electrolytes with varying Cs⁺ concentrations in Li₂SO₄ background electrolyte (pH 3, total cation concentration: 0.1 M). The activity was determined by re-oxidation of produced CO. Reprinted with permission from Monteiro et al. [70]. Copyright (2021) Springer Nature Limited. (B) CO partial current density and faradaic efficiencies (FE) for CO₂-to-CO conversion on polycrystalline Ag electrodes at -0.94 V_{RHE} in 0.1 M bicarbonate electrolytes at near neutral pH as indicated. pDDA⁺: poly(dimethyl diallyl ammonium); TEA⁺: tetraethyl ammonium. Reprinted with permission from Weng et al. [71]. Copyright (2023) American Chemical Society.

found that detectable amounts of CO are only formed in the presence of alkali cations. The CO₂-to-CO conversion activity at pH 3 with 1 mM alkali cations correlates with hydrated cation size, which an analysis of AIMD simulations shows increases from Li⁺ to Cs⁺. At a fixed total alkali cation concentration (0.1 M) with Li₂SO₄ as the background electrolyte, they determined that increasing the concentration of Cs⁺ ions from 0 to 1 mM steeply increases the amount of CO produced (Fig. 6A). On the basis of these findings and AIMD simulations, they attributed the activity trend to the increasing propensity of the alkali cation to accumulate in the OHP and to coordinate to adsorbed CO₂⁻ when going from Li⁺ to Cs⁺. The coordination results in electrostatic stabilization of the CO₂⁻ intermediate.

In a related study, Monteiro et al. examined the effects of multivalent cations on CO_2 reduction.³⁴ Their effect changes with applied electrode potential. At low overpotential (e.g., $\approx -0.45~\mathrm{V}_\mathrm{RHE}$), multivalent cations tend to enhance CO_2 reduction relative to the rates in the presence of monovalent cations. At high overpoten-

tial $(e.g., \approx -1.00 \text{ V}_{\text{RHE}})$, monovalent cations give rise to higher CO₂ reduction rates than multivalent ones. Monteiro et al. explained these observations by the effect of the cations on the competing HER (section IIA). In the low overpotential regime, proton reduction is the primary competing reaction, which is largely unaffected by the identity of the cation. AIMD simulations (with a low cation coverage of 0.07 monolayers) suggest that multivalent and weakly hydrated cations (Ba²⁺ and Nd³⁺) more stably coordinate to surface-adsorbed CO_2^- . The resulting short- and medium-range electrostatic interactions stabilize the CO_2^- intermediate, thereby promoting the reduction reaction. By contrast, at higher overpotentials, multivalent cations more strongly promote the competing water reduction reaction relative to CO₂ reduction (as discussed in section IIA). Taken together, the effect of the supporting electrolyte's cation on the competition between the HER and CO₂ reduction is the net result of at least three factors: Its accumulation in the OHP, its ability to stabilize the CO_2^- intermediate through coordination, and its effect on the competing HER.

Monteiro et al.'s results demonstrate that a cation other than H₃O⁺ is necessary for CO₂ reduction.⁷⁰ A key question is whether that cation needs to engage in a coordinative interaction with CO₂ to facilitate the reaction. 56,70,72 Weng et al. showed that CO₂-to-CO conversion also occurs in the presence of weakly coordinating organic cations.⁷¹ For example, on polycrystalline Au at -0.75 V_{RHE} in 0.1 M (ethyl)₄N(HCO₃), they observed a CO partial current of 1.6 mA cm⁻². Although $\sim 40\%$ lower than the reduction current observed in 0.1 M NaHCO₃ under otherwise identical conditions, this result demonstrates that CO production occurs at substantial rates in the presence of $(ethyl)_4N^+$. On a polycrystalline Ag electrode at $-0.80 \text{ V}_{\text{RHE}}$, the CO partial current is 0.5 mA cm⁻² in 0.1 M (ethyl)₄N(HCO₃) and 0.1 M NaHCO₃. In the presence of poly(dimethyl diallyl ammonium), Ag exhibits essentially the same CO₂ reduction activity as in Cs⁺-containing electrolyte (Fig. 6B). Weng et al. took great care to exclude the possibility that the activity arises from traces of alkali metal cations in the electrolytes with the organic cations. Taken together, these results demonstrate that although cations other than H_3O^+ need to be present for CO_2 reduction to occur, the cation does need to be a coordinating one for the reaction to proceed.

The studies discussed in the preceding paragraphs did not experimentally analyze the distribution and properties of the EDL. In the following, we summarize several key studies focused on experimentally elucidating the properties of the electrocatalytic interface under reaction conditions.

Ovalle *et al.* probed the accumulation of alkali metal cations at the Au/electrolyte interface during ${\rm CO_2}$ reduction with SEIRAS using tetramethylammonium (methyl₄N⁺) as a vibrational reporter.⁶⁷ They established that the asymmetric ${\rm CH_3}$ deformation mode of

methyl₄N⁺ shifts from ~ 1490 cm⁻¹ to ~ 1482 cm⁻¹ upon specific adsorption. Addition of K⁺ to the electrolyte at a fixed electrode potential decreases the absorbance at 1482 cm⁻¹ (Fig. 7A), suggesting a displacement reaction of the form:

$$\operatorname{methyl}_4 N_{\operatorname{ads}} + K_{\operatorname{aq}}^+ + \delta e^- \to \operatorname{methyl}_4 N_{\operatorname{aq}}^+ + K_{\operatorname{ads}}, \quad (1)$$

where δe^- represents an increment of electronic charge. The adsorbed cations retain a significant fraction of their positive charge, which for simplicity is not explicitly shown in equation 1. Equation 1 implies that the loss of absorbance at 1482 cm⁻¹ is a relative measure of the amount of specifically adsorbed K⁺. Ovalle et al. showed that the relative amounts of specifically adsorbed alkali cations at a fixed bulk concentration is determined by their free energy of hydration (Fig. 7B). Further, the rate of CO₂ reduction monotonically increases with the amount of specifically adsorbed cations at $-0.45~\rm V_{RHE}$. This observation provides a rationale for the higher rate of CO₂-to-CO conversion in the series Li⁺<Na⁺<K⁺<Cs⁺, but does not uniquely identify a mechanism.

Zhu et al. measured interfacial electric fields at the Au/electrolyte interface during CO₂-to-CO conversion with plasmon-enhanced vibrational sum frequency generation (VSFG) spectroscopy.⁶⁴ They showed that CO₂ reduction activity is closely related to the Onsager reaction field rather than the Stern field. Using in-situ generated CO on Au during CO₂ reduction as a vibrational Stark reporter, they selectively probed the interfacial electric field at catalytically active sites on Au as a function of cation identity and electrode potential. The Onsager reaction field arises from the polarization of the dielectric environment (electrolyte) by the dipolar solute (adsorbed CO).⁶³ The vibrational shift of adsorbed CO when going from the vacuum to the electrolyte environment (at the potential of zero charge of the electrode) is proportional to the magnitude of the Onsager reaction field. Zhu et al.'s analysis shows that the absolute magnitude of the Onsager reaction field increases from Li⁺ to Rb⁺ (Fig. 7C). They attributed this observation to the modulation of the interfacial dielectric constant by the cations. The Stern field arises from the polarization of the electrode and depends on the applied potential and EDL width. Its absolute magnitude increases from Rb⁺ to Li⁺. This observation suggests that the EDL width is thinner in the presence of Li⁺ than in Rb⁺containing electrolyte, consistent with the crystal radii of the cations. Cs⁺ represents an exception from these trends, indicating that it specifically adsorbs on the electrode, which is also reflected in a distinct interfacial water structure. The Onsager reaction field and CO₂ reduction rate show a correlation. The Onsager reaction field experienced by adsorbed CO₂⁻ is predicted to exceed the Stern field by one order of magnitude.

Using VSFG spectroscopy, Rebstock *et al.* probed the hydration of alkali cations at catalytically active and inactive sites on Au electrodes. 73 During CO₂ reduction, a

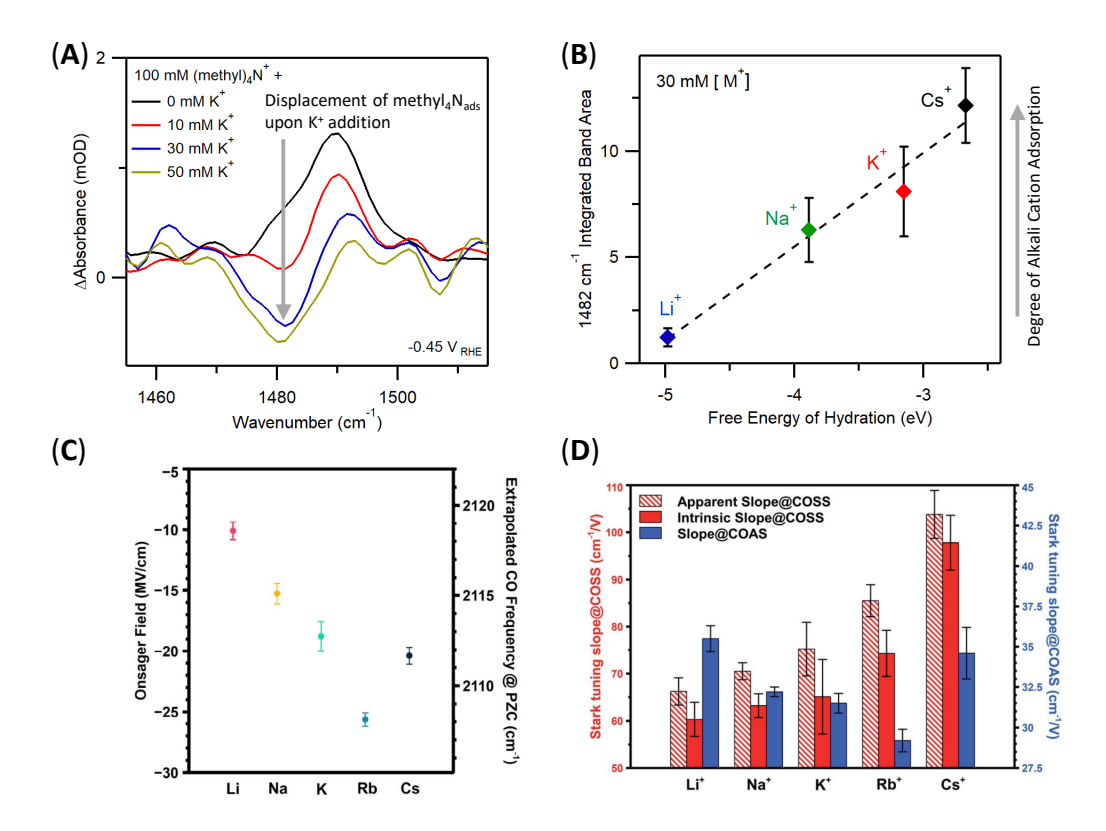


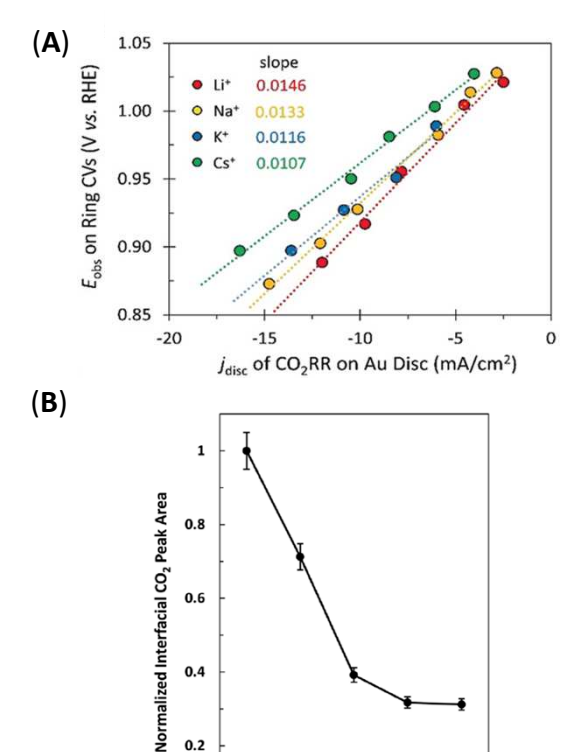
FIG. 7. Interfacial Accumulation of Cations and Cation-Dependent Interfacial Fields. (A) SEIRA spectra of the Au/aqueous electrolyte interface at an electrode potential of $-0.45 \, \rm V_{RHE}$. Addition of K⁺ to a 0.1 M methyl₄N⁺ bicarbonate electrolyte decreases the absorbance at 1482 cm⁻¹. The decrease is attributable to the displacement of methyl₄N_{ads} by K_{ads}. The bulk concentrations of K⁺ are indicated in the legend. (B) Correlation of the integrated area of the 1482 cm⁻¹ band with the hydration free energy of the cations. Decreasing band area indicates a higher degree of specific alkali cation adsorption. The bulk concentration for the alkali cations [M⁺] was 30 mM. The electrode potential was $-0.45 \, \rm V_{RHE}$. Panels (A) and (B) adapted with permission from Ovalle et al. [67]. Copyright (2022) Springer Nature Limited. (C) Onsager reaction field (left axis) induced by atop-bound CO on polycrystalline Au in 0.1 M bicarbonate electrolytes as indicated. The Onsager field was derived from the extrapolated CO frequencies at the potential of zero charge (PZC) of the electrode (right axis). Reprinted with permission from Zhu et al. [64] Copyright (2022) The Authors. Published by the American Chemical Society. (D) Stark tuning slopes of atop-bound CO on Au electrodes in 0.1 M bicarbonate electrolytes as indicated. The steeper the slope, the higher the interfacial field. COSS: CO on spectator site (terrace site); COAS: CO on active site (undercoordinated Au site). At high surface concentrations of CO dynamic dipole coupling affects to observed slope. The apparent Stark tuning slope is the one experimentally observed. The intrinsic Stark tuning slope is corrected for dynamic dipole coupling. Reprinted with permission from Rebstock et al. [73] Copyright (2022) The Authors. Published by the Royal Society of Chemistry.

single CO stretch band at $\sim 2100~\rm cm^{-1}$ appears. They demonstrated that this band arises from CO adsorbed on catalytically active sites (undercoordinated minority sites, comprising at most 4% of surface sites). By contrast, with CO-saturated electrolytes an additional band at $\sim 2090~\rm cm^{-1}$ appears, which is attributable to CO adsorbed on catalytically inactive sites (terrace sites).

The potential-dependent VSFG spectra reveal that the CO stretch bands of the two populations exhibit distinct Stark tuning slopes, which measure the sensitivity of the CO stretch frequency to the applied electrode potential (Fig. 7D). The Stark tuning slope of CO adsorbed on catalytically active sites decreases when going from Li⁺to Rb⁺-containing electrolyte. By contrast, the slope of CO on inactive sites exhibits the opposite trend. Analysis of the Stark tuning slopes in the framework of Gouy-

Chapman-Stern theory reveals that the Stern-layer thickness at inactive sites closely tracks the hydration radius of the ions as determined from ion mobility measurements (Stokes radii), changing from 6.7 (Li⁺) to 4.1 (Rb⁺) Å. By contrast, the Stern layer width at catalytically active sites exhibits the opposite trend, increasing from Li⁺ (3.4 Å) to Rb⁺ (4.0 Å), suggesting that only a single layer of water molecules between cation and Au surface is retained at these sites. This study highlights that catalytically active sites may exhibit a distinct local hydration structure compared with inactive majority sites. The correlation between site-specific hydration structure and catalytic activity demonstrates the importance of understanding the local solvation structure.

Apart from influencing the EDL structure, alkali cations have been suggested to modulate the interfacial



0.2

0

Li Na

FIG. 8. Effect of Cations on Interfacial CO₂ Concentration and pH. (A) Observed peak potential of CO oxidation (E_{obs}) on the Pt ring electrode as a function of CO_2 reduction current on the Au disk in 0.1 M bicarbonate electrolytes as indicated. The steeper the slope, the higher the interfacial pH, which can be quantitatively extracted from the measurements. Reprinted with permission from Zhang et al. [74]. Copyright (2020) Wiley-VCH Verlag GmbH & Co. KGaA, Weinheim. (B) Normalized band area of the asymmetric stretch mode of interfacial CO₂ at a polycrystalline Au electrode at $-0.8 \text{ V}_{\text{RHE}}$ in 0.25 M bicarbonate electrolytes as indicated. The normalized band area is proportional to the interfacial concentration of CO₂. Reprinted with permission from Malkani et al. [75]. Copyright (2020) American Chemical Society.

Rb

Cs

pH during catalysis. ⁷⁶ It has been hypothesized that the pH buffering effect by alkali cations may control the availability of CO_2 at the interface.

Zhang et al. assessed the local pH in the vicinity of a polycrystalline Au electrode in bicarbonate buffer during CO₂-to-CO conversion with a rotating ring-disk electrode.⁷⁴ The reduction of CO₂ on the disk produces CO and OH⁻, which convectively diffuse to the Pt ring electrode, where CO is oxidized. Their method quantifies the pH through the potential of the CO oxidation peak current on the Pt ring electrode. This potential is pHdependent and, after calibration, can be quantitatively related to the local pH. They found that the potential

corresponding to the CO oxidation peak current exhibits a steeper decrease with CO₂ reduction current density in the presence of Li⁺ than in Cs⁺-containing electrolyte (Fig. 8A). This result indicates that at a CO₂ reduction current density of 10 mA cm⁻², the local pH in Li⁺-containing electrolyte is about 0.5 pH units higher than in Cs⁺-containing electrolyte. These observations demonstrate that alkali metal cations buffer the interfacial pH to different extents, as previously predicted.⁷⁶ However, these and prior measurements⁷⁷ did not assess the effect on the interfacial ${\rm CO}_2$ concentration.

Malkani et al. directly measured the relative concentrations of dissolved CO₂ within a few nanometers of an Au electrode during CO₂-to-CO conversion with SEIRAS. 75 They found that the interfacial CO_2 concentration at $-0.8~V_{RHE}$ decreases by $\sim 70\%$ when going from Li⁺- to Cs⁺-containing electrolyte (Fig. 8B). This decrease closely mirrors the increase in CO₂ partial current density with increasing crystal radius of the cation. This result suggests that the rate of CO₂ conversion rather than the cation-dependent pH buffer capacity determines the local CO₂ concentration. This interpretation is further supported by constant-current electrolysis, where OH⁻ is generated at a constant rate across different electrolytes. If the cation-dependent pH buffer capacity predominately determined the interfacial CO₂ concentration, a higher concentration would be expected in the presence of Cs⁺ than in Li⁺-containing electrolyte. However, Malkani et al. observed the opposite trend at a current density of -1.77 mA cm^{-2} , indicating that the cation-dependent rate of CO₂-to-CO conversion primarily dictates the interfacial concentration of CO_2 .

Critical Assessment

Before we evaluate the different possible mechanisms of CO_2 promotion, we first analyze the current understanding of the accumulation and distribution of alkali cations in the EDL.

1. Accumulation and Distribution of Alkali Cations in the **EDL**

Ovalle et al. demonstrated with SEIRAS that the degree to which alkali metal cations displace tetramethylammonium at the aqueous Au interface at -0.45 V_{RHE} correlates with their free energy of hydration.⁶⁷ The softer the hydration shell of the alkali cation, the higher the tendency for its interfacial accumulation. This trend is not limited to electrolytes containing 0.1 M tetramethylammonium bicarbonate (pH 6.8). Monteiro et al.'s observation that the CO₂ reduction activity steeply increases by addition of small amounts of Cs^+ to ~ 0.1 M Li⁺containing electrolyte at pH 3 strongly suggests that Cs⁺ has a higher affinity for the interface than Li⁺. ⁷⁰ Similarly, Bender et al. showed that low concentrations of K⁺

and Cs^+ in 0.1 M LiOH give rise to HER activities on Pt electrodes comparable to those in pure 0.1 M KOH or CsOH.³⁶ Shah *et al.* showed with ETS that alkali cation accumulation on Pt electrodes increases with softer hydration shell. These trends are also reproduced by AIMD simulations.⁴² Taken together, the trend that alkali metal cation accumulation in the double layer increases from Li^+ to Cs^+ appears to be robust across different metals and electrolyte compositions.

We next address the question in regards to the physical cause of the differential accumulation of alkali cations. As detailed below, there are at least three hypotheses in regards to the differential interfacial enrichment: Steric repulsion between hydration shells, specific adsorption, and quasi-specific adsorption mediated by anions at the interface. Because all three mechanisms are strongly influenced by the free energy of hydration of the cation, it is challenging to experimentally distinguish between them.

The extent of steric repulsion between the hydration shells of alkali metal cations may determine their interfacial concentrations. Ringe et al. demonstrated this concept on the basis of a Poisson-Boltzmann model that accounts for the finite sizes of the hydrated cations, assuming that interfacial Cs⁺ has a smaller hydrated radius than Li⁺. ⁷⁸ This assumption may appear surprising given that molecular dynamics simulations and X-ray scattering indicate that the bulk hydration radius increases from Li⁺ to Cs⁺.⁴¹ However, Stark effect measurements show that the effective hydration radii of cations at electrode interfaces do not always follow this trend. 64,73,79,80 On the basis of AIMD simulations, Monteiro et al. argued that partial dehydration minimizes steric repulsion between cations, thereby facilitating the accumulation of cations with softer hydration shells.³⁴

The steric repulsion hypothesis is primarily based on the interpretation of AIMD simulations and modified Poisson-Boltzmann models with demonstrated success in predicting catalytic rates.^{34,78} It would be desirable to design experiments that more directly test the repulsion between hydrated cations. Designing such experiments is challenging but likely not impossible. For example, Wallentine et al. probed the Stark shift of CO adsorbed on catalytically active sites on polycrystalline Au electrodes in contact with CO₂-saturated 0.1 M sodium bicarbonate electrolyte.⁵⁴ They found that the Stark shift of the CO stretch vibration of adsorbed CO linearly decreases with applied potential, but reaches a saturation value at \sim -0.7 V_{SHE}. This result suggests the formation of a dense cation layer at this potential, thereby saturating the Stern electric field. It would be interesting to test whether the threshold potential depends on the hydration free energy of the cation.

Alkali cation enrichment may be driven by specific adsorption, which is facilitated by partial dehydration. Specific adsorption of alkali cations necessitates partial dehydration and is characterized by partial electron transfer from the electrode to the cation.⁸¹ Ovalle *et al.*⁶⁷ pre-

sented strong circumstantial evidence for specific alkali cation adsorption on Au at -0.45 V_{RHE}, which includes the findings that (1) the extent of $methyl_4N_{ads}$ displacement by alkali cations correlates with their hydration free energy, (2) the CO₂ reduction rate increases with the degree of methyl₄N_{ads} displacement, and (3) DFT calculations predict the specific adsorption of alkali cations at the relevant potentials. Although the idea of specific adsorption of alkali cations other than Cs⁺ remains controversial, there appears to be a broad consensus that Cs⁺ tends to specifically adsorb: In comparison with electrolytes containing 0.1 M LiOH, NaOH, or KOH, Shah et al. observed a substantially flattened ETS curve with electrode potential in their experiments with Pt electrodes in 0.1 M CsOH.⁴² Because ETS probes surfaceadsorbed species, this result suggests that Cs⁺ specifically adsorbs. Zhu et al. noted that the Onsager field (induced by adsorbed CO) monotonically decreases from Li⁺ to Rb⁺, but this trend is broken for Cs⁺.⁶⁴ Additionally, the O-H stretch spectrum of interfacial water in the presence of Cs⁺ is distinct from that observed in the presence of the other alkali cations. The authors of these studies attributed these observations to the specific adsorption of Cs⁺ under the respective conditions.

Anions at the interface may promote the enrichment of cations. The ETS experiments of Shah *et al.* indicate that the interaction of alkali cations with adsorbed hydroxide on the Pt electrode determines the interfacial cation concentration. ⁴² These cations are best described as quasi-specifically adsorbed. The role of anions in mediating cation enrichment has also been observed in many other systems and has been discussed in our earlier perspective. ¹⁰

We now address the question where in the EDL the cations preferentially reside. The average surface-cation distance determines the interfacial field and the cation's interaction with surface intermediates. An agreement on the average distance of the cations from the electrode surface has yet to emerge. AIMD simulations by Monteiro et al. indicate that the cation-surface distance on Au correlates with the ionic crystal radius, that is, it increases when going down the alkali metal group.³⁴ By contrast, the size-modified Poisson-Boltzmann model of Ringe et al. places Rb⁺ closer to the electrode than Li⁺.⁷⁸ The effective interfacial radii were extrapolated from the values of Cs⁺ and K⁺ determined by surface X-ray scattering on Au(111), under the assumption that the radii are insensitive to applied potential and identity of the metal surface. Indeed, Stark spectroscopy suggests that the interfacial field experienced by atop-bound CO on Cu and Au terrace sites and on polycrystalline Pt increases in the order Li⁺, Na⁺, K⁺, Rb⁺ (suggesting a decreasing Stern layer width). 64,73,79,80 However, the opposite trend holds for CO adsorbed on undercoordinated sites of Au, which are catalytically active for CO₂ reduction.⁷³ These results suggest that the approach of alkali cations is dependent upon the local surface structure around the active site. It is therefore preferable to adopt a local picture when

examining cation effects.

2. Promotion Mechanisms

Having discussed the current understanding of interfacial cation accumulation and distribution in the EDL, we now examine how interfacial alkali cations can influence CO_2 conversion. As noted at the beginning of section III, the stabilization of adsorbed CO_2^- (and the transition state leading to it) is commonly accepted as the principal reason of the promotion of CO_2 -to-CO conversion. Different mechanisms for the stabilization have been proposed and are debated in the literature. In the following, we discuss those mechanisms.

In the first picture (Fig. 9A/B), stabilization arises from Lewis acid-base interaction between cation (Lewis acid) and adsorbed CO_2^- (Lewis base). The energy stabilization of the cation- CO_2^- adduct as a result of Lewis acid-base interaction can be thought of as arising from the sum of two terms:^{82,83}

$$\Delta E = \Delta E_{\text{Coulomb}} + \Delta E_{\text{dative}},$$
 (2)

where $\Delta E_{\text{Coulomb}}$ and ΔE_{dative} represent the stabilization due to Coulomb interaction and dative bond formation, respectively (An electronic repulsion term, which is sometimes included in the sum, is neglected here). The Coulomb term represents ion-ion (or dipole-ion) interaction without charge-transfer. By contrast, ΔE_{dative} represents (partial) electron transfer from the Lewis base to the Lewis acid, which results in the formation of a (partial) coordinate covalent bond. Within the Lewis acidbase framework, zero electron transfer (pure Coulomb interaction, Fig. 9B) and full transfer of one or more electrons (dative bond formation, Fig. 9A) are the extremes of a continuum of degrees of electron donation. A key question is whether the stabilization of CO₂ involves the formation of a (partial) coordinate covalent bond between this intermediate and an alkali cation. Partial coordinate covalent bond formation is expected to have a more pronounced effect on the stability of the intermediate than the comparatively weaker Coulomb interac $tion.^{83}$

Monteiro et al.'s results demonstrate that alkali cations enable CO_2 -to-CO conversion, whereas $\mathrm{H}_3\mathrm{O}^+$ cannot. On principle, alkali cations can participate in both types of interactions described by the two terms in equation 2. However, Weng et al. found that some non-coordinating organic cations can give rise to CO_2 reduction activity comparable to that in the presence of alkali cations. Non-coordinating organic cations are unlikely to form a (partial) coordinate covalent bond with CO_2^- . Therefore, the $\Delta E_{\mathrm{dative}}$ term is expected to be insignificant in this case. When viewed collectively, these observations suggest that alkali and (some) organic cations stabilize the intermediate through the Coulomb term in equation 2 ($\Delta E_{\mathrm{Coulomb}}$) and dative bond formation is negligible in both cases. This interpretation is also consis-

tent with computational studies. Chen et al. calculated the cation-induced stabilization of CO₂ on Ag electrodes with DFT. They found that the DFT-predicted stabilization can be described by the interaction of the intermediate's dipole/polarizability with the cation-induced electric field, indicating that specific chemical bonding effects are negligible.⁸⁴ Monteiro et al.'s analysis of their AIMD simulations also showed that the stabilization can be estimated on the basis of the interaction of the intermediate's dipole with the electric field at the adsorption site.⁷⁰ Taken together, alkali and some non-coordinating organic cations appear to stabilize CO_2^- primarily through the Coulomb term in equation 2. The electric field produced at the adsorption site is of course influenced by specific chemical interactions between electrolyte components, surface intermediates, and the electrode surface. Therefore, even weak chemical interactions may be essential for producing the requisite electric field for CO₂ reduction at the active sites.

Another important question is whether the electrostatic stabilization can be described by the mean electric field predicted by classical EDL theory (Fig. 9C) or if the local field at the active site (Fig. 9B) needs to be consid- ${
m ered.}^{8,71}$ Classical EDL theory assumes a spatially and temporally homogeneous field. 85 Using surface-adsorbed CO as a molecular electric field probe, Rebstock et al. showed that the magnitude of the electric field at different types of surface sites can be significantly different and can exhibit opposite trends with respect to the crystal radius of the alkali cation.⁷³ We note that the following factors could also contribute to the apparent sitedependence: Changes in the CO_{ads} coverage may affect the interfacial solvation structure. Further, CO_{ads} on terrace sites and $\mathrm{CO}_{\mathrm{ads}}$ on step sites are stable in different potential windows. A potential-dependence of the Stark slope cannot be fully excluded. Irrespective, these results indicate that it is important to consider the local electric field whenever possible. This view is also supported by calculations. For example, using DFT calculations, Chen et al. demonstrated the lateral heterogeneity of the electric field.⁸⁴ Similarly, Monteiro et al.'s AIMD simulations showed that the large field in the immediate proximity of the cation is necessary to facilitate CO_2 reduction.³⁴

Apart from interacting with the Stern field, CO_2^- can also induce an Onsager reaction field, which in turn stabilizes the intermediate (Fig. 9D). Zhu et~al. estimated that the strength of the Onsager field (experienced by CO_2^-) substantially exceeds that of the Stern field. It would be interesting to extend this study to other electrolytes, such as those containing organic cations, or highly concentrated electrolytes. Such studies would help to ascertain further the role of the Onsager field in facilitating electrocatalytic processes that feature reaction intermediates with large dipole moments.

Lastly, we examine the question whether hydrated alkali cations influence the local CO₂ concentration through pH buffering effects (Fig. 9E). The measurements by Zhang *et al.* unequivocally demonstrate

(A) Dative Bond Formation (B) Local Coulomb Interaction (C) Dipole/EDL Field Interaction

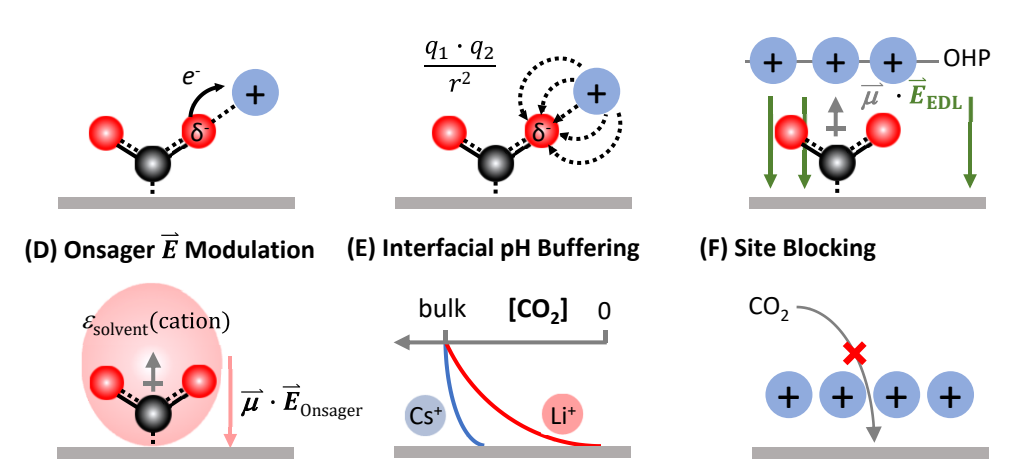


FIG. 9. Cartoon Representations of Proposed Effects of Cations on CO_2 Reduction. (A) Dative bond formation between adsorbed CO_2 , represented by black (carbon) and red (oxygen) spheres, and the cation (blue circle). e^- and the arrow illustrate (partial) electron transfer. (B) Local electrostatic interaction between the dipole/polarizability of adsorbed CO_2 and the local electric field produced by the cation. The dashed lines with arrows represent electric field lines. Coulomb's law is shown to illustrate the difference of this view to the charge-transfer picture shown in panel (A). (C) Stabilization of adsorbed CO_2 by the interaction of its dipole moment ($\vec{\mu}$) and/or polarizability with the EDL electric field (\vec{E}_{EDL}). The green and gray arrows illustrate \vec{E}_{EDL} and $\vec{\mu}$, respectively. (D) Modulation of the interfacial dielectric constant ($\varepsilon_{solvent}$) by cations in the EDL alters the Onsager reaction field ($\vec{E}_{Onsager}$), which in turn acts on the dipole moment/polarizability of adsorbed CO_2 . (E) Hydrated alkali cations can buffer the interfacial pH, thereby changing the local CO_2 concentration. The lines illustrate the hypothetical change in CO_2 concentration as a function of distance from the electrode in the presence of different cations. (F) The formation of a compact EDL blocks CO_2 (and/or H_3O^+) from accessing active sites.

that the local pH during CO₂-to-CO reduction depends on cation identity and is lower in Cs⁺- than in Li⁺containing electrolyte.⁷⁴ However, the differences in local pH appear rather moderate and Malkani et al.'s results demonstrate that the primary determinant of the interfacial CO₂ concentration is the reaction rate rather than the different buffer capacities of the cations.⁷⁵ We therefore conclude that the hydrolysis of hydrated alkali cations does not play a major role in enhancing CO₂ reduction in H-cells (the situation may be different in gas diffusion electrodes). The hydrolysis of multivalent cations appears to play a role in promoting HER under certain conditions.³⁴ We also note that electrocatalytic reactions are often highly sensitive to the local pH (and vice versa). 86–88 Several methods for measuring the local pH have been summarized in a recent review⁸⁹.

IV. CONCLUSIONS AND OUTLOOK

Substantial progress has been made in identifying potential mechanisms by which cations influence the HER (Fig. 5) and CO₂-to-CO conversion (Fig. 9). Although the relative weight of the proposed mechanisms cannot be conclusively assessed at this time, the collective evidence suggests some scenarios as more probable than others. For HER promotion by cations, we favor a combination of two mechanisms: The stabilization of the tran-

sition state energy through water-cation interactions and cation-induced changes in the collective dynamics of the interface. However, other mechanisms may also make important contributions to the promotion of the HER. For $\rm CO_2$ reduction, we feel that the models that picture the promotion as arising from electrostatic stabilization of the $\rm CO_2^-$ intermediate (and the transition state leading to it) are most consistent with the experimental and theoretical evidence (Fig. 9B-D). A site-specific view of the electric field appears most appropriate. Yet, further investigations are required to determine which of the proposed electrostatic stabilization models provides a satisfactory description for explaining observed reactivity trends.

There is also evidence that alkali cations can inhibit the HER and CO₂-to-CO conversion under certain conditions (Fig. 9F). This regime remains underexplored, especially in regards to an analysis of the interface. Further characterization of the inhibition effects is important because practical electrolyzers typically operate at high concentrations of alkali cations (1 to several mols/L).^{90,91} More generally, it would be important to systematically explore cation effects in the context of gas diffusion electrodes. The reaction conditions in these electrodes can give rise to unintended effects of cations on electrolyzer performance.^{92,93}

The progress in understanding cation effects has been enabled by advanced electrochemical experimentation, in

situ and operando interfacial measurements, and theoretical models and computer simulations of electrocatalytic interfaces. It is this combination and the tight integration of these methods of investigation that are key toward making further strides in advancing and refining this understanding. A key challenge is that cations affect a multitude of interrelated properties of the interface. Assessing the relative impact of these changes on catalysis cannot be solely achieved with experiments. Measurements of interfacial properties are essential for benchmarking models, which can help evaluate how a certain change affects key steps in an electrocatalytic process. The studies described in this perspective provide a rich knowledge framework and inspiration for future work.

ACKNOWLEDGMENTS

We thank Professor Alexis Grimaud for helpful discussions. This work was supported by the National Science Foundation through a CAREER award (Award No. CHE-1847841).

- ¹C. Tang, Y. Zheng, M. Jaroniec, and S.-Z. Qiao, "Electrocatalytic refinery for sustainable production of fuels and chemicals," Angew. Chem. Inter. Ed. 60, 19572–19590 (2021).
- ²J. Sisler, S. Khan, A. H. Ip, M. W. Schreiber, S. A. Jaffer, E. R. Bobicki, C.-T. Dinh, and E. H. Sargent, "Ethylene electrosynthesis: A comparative techno-economic analysis of alkaline vs membrane electrode assembly vs CO₂-CO-C₂H₄ tandems," ACS Energy Lett. 6, 997–1002 (2021).
- ³H. Shin, K. U. Hansen, and F. Jiao, "Techno-economic assessment of low-temperature carbon dioxide electrolysis," Nat. Sustain. 4, 911–919 (2021).
- ⁴US Department of Energy, Office of Science (SC), Basic Energy Sciences (BES), Washington DC (United States), "Basic energy sciences roundtable: Foundational science for carbon-neutral hydrogen technologies," BES Reports (2021), 10.2172/1822215.
- ⁵P. J. Rheinländer, J. Herranz, J. Durst, and H. A. Gasteiger, "Kinetics of the hydrogen oxidation/evolution reaction on polycrystalline platinum in alkaline electrolyte reaction order with respect to hydrogen pressure," J. Electrochem. Soc. **161**, F1448 (2014).
- ⁶N. Dubouis and A. Grimaud, "The hydrogen evolution reaction: from material to interfacial descriptors," Chem. Sci. **10**, 9165–9181 (2019).
- ⁷J. E. Huang, F. Li, A. Ozden, A. Sedighian Rasouli, F. P. García de Arquer, S. Liu, S. Zhang, M. Luo, X. Wang, Y. Lum, Y. Xu, K. Bertens, R. K. Miao, C.-T. Dinh, D. Sinton, and E. H. Sargent, "CO₂ electrolysis to multicarbon products in strong acid." Science **372**, 1074–1078 (2021).
- ⁸J. Gu, S. Liu, W. Ni, W. Ren, S. Haussener, and X. Hu, "Modulating electric field distribution by alkali cations for CO₂ electroreduction in strongly acidic medium," Nat. Catal. 5, 268–276 (2022).
- ⁹M. Dunwell, Y. Yan, and B. Xu, "Understanding the influence of the electrochemical double-layer on heterogeneous electrochemical reactions," Curr. Opin. Chem. Engineer. 20, 151–158 (2018).
- ¹⁰M. M. Waegele, C. M. Gunathunge, J. Li, and X. Li, "How cations affect the electric double layer and the rates and selectivity of electrocatalytic processes," J. Chem. Phys. **151**, 160902 (2019).
- ¹¹O. M. Magnussen and A. Groß, "Toward an atomic-scale under-standing of electrochemical interface structure and dynamics," J. Am. Chem. Soc. **141**, 4777–4790 (2019).

- ¹²S. Banerjee, X. Han, and V. S. Thoi, "Modulating the electrode– electrolyte interface with cationic surfactants in carbon dioxide reduction," ACS Catal. 9, 5631–5637 (2019).
- ¹³F. Kiguchi, M. Nakamura, and N. Hoshi, "Cation effects on ORR activity on low-index planes of Pd in alkaline solution," Electrochemistry 89, 145–147 (2021).
- ¹⁴X. Ding, D. Scieszka, S. Watzele, S. Xue, B. Garlyyev, R. W. Haid, and A. S. Bandarenka, "A systematic study of the influence of electrolyte ions on the electrode activity," ChemElectroChem 9, e202101088 (2022).
- ¹⁵R. R. Rao, B. Huang, Y. Katayama, J. Hwang, T. Kawaguchi, J. R. Lunger, J. Peng, Y. Zhang, A. Morinaga, H. Zhou, H. You, and Y. Shao-Horn, "pH- and cation-dependent water oxidation on rutile RuO₂(110)," J. Phys. Chem. C **125**, 8195–8207 (2021).
- ¹⁶ J. Huang, M. Li, M. J. Eslamibidgoli, M. Eikerling, and A. Groß, "Cation overcrowding effect on the oxygen evolution reaction," JACS Au 1, 1752–1765 (2021).
- ¹⁷N. C. Kani, A. Prajapati, B. A. Collins, J. D. Goodpaster, and M. R. Singh, "Competing effects of pH, cation identity, H₂O saturation, and N₂ concentration on the activity and selectivity of electrochemical reduction of N₂ to NH₃ on electrodeposited Cu at ambient conditions," ACS Catal. 10, 14592–14603 (2020).
- ¹⁸V. Briega-Martos, F. J. Sarabia, V. Climent, E. Herrero, and J. M. Feliu, "Cation effects on interfacial water structure and hydrogen peroxide reduction on Pt(111)," ACS Meas. Sci. Au 1, 48–55 (2021).
- ¹⁹B. A. F. Previdello, E. G. Machado, and H. Varela, "The effect of the alkali metal cation on the electrocatalytic oxidation of formate on platinum," RSC Adv. 4, 15271–15275 (2014).
- ²⁰C. J. Bondue and M. T. M. Koper, "A mechanistic investigation on the electrocatalytic reduction of aliphatic ketones at platinum," J. Catal. 369, 302–311 (2019).
- ²¹P. Herasymenko and I. Šlendyk, "Wasserstoff Überspannung und Adsorption der Ionen," Z. Phys. Chem. A **149**, 123–139 (1930).
- ²²A. Frumkin, "Wasserstoffüberspannung und Struktur der Doppelschicht," Z. Phys. Chem. **164A**, 121–133 (1933).
- ²³A. N. Frumkin, "Influence of cation adsorption on the kinetics of electrode processes," Trans. Faraday Soc. **55**, 156–167 (1959), http://dx.doi.org/10.1039/TF9595500156.
- ²⁴M. T. M. Koper, "Theory and kinetic modeling of electrochemical cation-coupled electron transfer reactions," J. Solid State Electrochem. (2023), 10.1007/s10008-023-05653-0.
- ²⁵P. Sebastián-Pascual, Y. Shao-Horn, and M. Escudero-Escribano, "Toward understanding the role of the electric double layer structure and electrolyte effects on well-defined interfaces for electrocatalysis," Curr. Opin. Electrochem. 32, 100918 (2022).
- ²⁶S. Ringe, "Cation effects on electrocatalytic reduction processes at the example of the hydrogen evolution reaction," Curr. Opin. Electrochem. 39, 101268 (2023).
- ²⁷J. Wang, H.-Y. Tan, M.-Y. Qi, J.-Y. Li, Z.-R. Tang, N.-T. Suen, Y.-J. Xu, and H. M. Chen, "Spatially and temporally understanding dynamic solid–electrolyte interfaces in carbon dioxide electroreduction," Chem. Soc. Rev. 52, 5013–5050 (2023).
- ²⁸X. Wang, Q. Ruan, and Z. Sun, "Minireview of the electrocatalytic local environment in alkaline hydrogen evolution," Energy & Fuels 37, 17667–17680 (2023).
- ²⁹H. Khani, A. R. Puente Santiago, and T. He, "An interfacial view of cation effects on electrocatalysis systems," Angew. Chem. Inter. Ed. 62, e202306103 (2023).
- ³⁰A. Mathanker, W. Yu, N. Singh, and B. R. Goldsmith, "Effects of ions on electrocatalytic hydrogenation and oxidation of organics in aqueous phase," Curr. Opin. Electrochem. 40, 101347 (2023).
- ³¹P. Li, Y. Jiao, J. Huang, and S. Chen, "Electric double layer effects in electrocatalysis: Insights from ab initio simulation and hierarchical continuum modeling," JACS Au 3, 2640–2659 (2023).
- ³²M. A. Gebbie, B. Liu, W. Guo, S. R. Anderson, and S. G. Johnstone, "Linking electric double layer formation to electrocatalytic activity," ACS Catal. 13, 16222–16239 (2023).

- ³³S. Banerjee, C. S. Gerke, and V. S. Thoi, "Guiding CO₂RR selectivity by compositional tuning in the electrochemical double layer," Acc. Chem. Res. **55**, 504–515 (2022).
- ³⁴M. C. O. Monteiro, F. Dattila, N. López, and M. T. M. Koper, "The role of cation acidity on the competition between hydrogen evolution and CO₂ reduction on gold electrodes," J. Am. Chem. Soc. 144, 1589–1602 (2022).
- ³⁵M. C. O. Monteiro, A. Goyal, P. Moerland, and M. T. M. Koper, "Understanding cation trends for hydrogen evolution on platinum and gold electrodes in alkaline media," ACS Catal. 11, 14328–14335 (2021).
- ³⁶ J. T. Bender, A. S. Petersen, F. C. Østergaard, M. A. Wood, S. M. J. Heffernan, D. J. Milliron, J. Rossmeisl, and J. Resasco, "Understanding cation effects on the hydrogen evolution reaction," ACS Energy Lett. 8, 657–665 (2023).
- ³⁷A. Goyal and M. T. M. Koper, "The interrelated effect of cations and electrolyte pH on the hydrogen evolution reaction on gold electrodes in alkaline media," Angew. Chem. Int. Ed. **60**, 13452– 13462 (2021).
- ³⁸X. Chen, I. T. McCrum, K. A. Schwarz, M. J. Janik, and M. T. M. Koper, "Co-adsorption of cations as the cause of the apparent pH dependence of hydrogen adsorption on a stepped platinum single-crystal electrode," Angew. Chem. Inter. Ed. 56, 15025–15029 (2017).
- ³⁹L. Rebollar, S. Intikhab, J. D. Snyder, and M. H. Tang, "Determining the viability of hydroxide-mediated bifunctional HER/HOR mechanisms through single-crystal voltammetry and microkinetic modeling," J. Electrochem. Soc. 165, J3209 (2018).
- ⁴⁰E. Liu, J. Li, L. Jiao, H. T. T. Doan, Z. Liu, Z. Zhao, Y. Huang, K. M. Abraham, S. Mukerjee, and Q. Jia, "Unifying the hydrogen evolution and oxidation reactions kinetics in base by identifying the catalytic roles of hydroxyl-water-cation adducts," J. Am. Chem. Soc. 141, 3232–3239 (2019).
- $^{41}\mathrm{Y}.$ Marcus, "Ionic radii in aqueous solutions," Chem. Rev. 88, 1475-1498 (1988).
- ⁴²A. H. Shah, Z. Zhang, Z. Huang, S. Wang, G. Zhong, C. Wan, A. N. Alexandrova, Y. Huang, and X. Duan, "The role of alkali metal cations and platinum-surface hydroxyl in the alkaline hydrogen evolution reaction," Nat. Catal. 5, 923–933 (2022).
- ⁴³B. Huang, R. R. Rao, S. You, K. Hpone Myint, Y. Song, Y. Wang, W. Ding, L. Giordano, Y. Zhang, T. Wang, S. Muy, Y. Katayama, J. C. Grossman, A. P. Willard, K. Xu, Y. Jiang, and Y. Shao-Horn, "Cation- and pH-dependent hydrogen evolution and oxidation reaction kinetics," JACS Au 1, 1674–1687 (2021).
- ⁴⁴Y.-H. Wang, S. Zheng, W.-M. Yang, R.-Y. Zhou, Q.-F. He, P. Radjenovic, J.-C. Dong, S. Li, J. Zheng, Z.-L. Yang, G. Attard, F. Pan, Z.-Q. Tian, and J.-F. Li, "In situ Raman spectroscopy reveals the structure and dissociation of interfacial water," Nature 600, 81–85 (2021).
- ⁴⁵X. Ding, B. Garlyyev, S. A. Watzele, T. Kobina Sarpey, and A. S. Bandarenka, "Spotlight on the effect of electrolyte composition on the potential of maximum entropy: Supporting electrolytes are not always inert," Chemistry – A European Journal 27, 10016–10020 (2021).
- ⁴⁶P. Xu, R. Wang, H. Zhang, V. Carnevale, E. Borguet, and J. Suntivich, "Cation modifies interfacial water structures on platinum during alkaline hydrogen electrocatalysis," J. Am. Chem. Soc. 146, 2426–2434 (2024).
- ⁴⁷M. N. Jackson, O. Jung, H. C. Lamotte, and Y. Surendranath, "Donor-dependent promotion of interfacial proton-coupled electron transfer in aqueous electrocatalysis," ACS Catal. 9, 3737–3743 (2019).
- ⁴⁸G. Marcandalli, A. Goyal, and M. T. M. Koper, "Electrolyte effects on the faradaic efficiency of CO₂ reduction to CO on a gold electrode," ACS Catal. 11, 4936–4945 (2021).
- ⁴⁹A. Cuesta, "Measurement of the surface charge density of CO-saturated Pt(111) electrodes as a function of potential: the potential of zero charge of Pt(111)," Surf. Sci. 572, 11–22 (2004).
- ⁵⁰P. Li, Y. Jiang, Y. Hu, Y. Men, Y. Liu, W. Cai, and S. Chen,

- "Hydrogen bond network connectivity in the electric double layer dominates the kinetic pH effect in hydrogen electrocatalysis on Pt," Nat. Catal. 5, 900–911 (2022).
- ⁵¹N. Dubouis, A. Serva, E. Salager, M. Deschamps, M. Salanne, and A. Grimaud, "The fate of water at the electrochemical interfaces: Electrochemical behavior of free water versus coordinating water," J. Phys. Chem. Lett. 9, 6683–6688 (2018).
- ⁵²D. S. Venables, K. Huang, and C. A. Schmuttenmaer, "Effect of reverse micelle size on the librational band of confined water and methanol," J. Phys. Chem. B **105**, 9132–9138 (2001).
- ⁵³B. Huang, K. H. Myint, Y. Wang, Y. Zhang, R. R. Rao, J. Sun, S. Muy, Y. Katayama, J. Corchado Garcia, D. Fraggedakis, J. C. Grossman, M. Z. Bazant, K. Xu, A. P. Willard, and Y. Shao-Horn, "Cation-dependent interfacial structures and kinetics for outer-sphere electron-transfer reactions," J. Phys. Chem. C 125, 4397–4411 (2021).
- ⁵⁴S. Wallentine, S. Bandaranayake, S. Biswas, and L. R. Baker, "Direct observation of carbon dioxide electroreduction on gold: Site blocking by the Stern layer controls CO₂ adsorption kinetics," J. Phys. Chem. Lett. **11**, 8307–8313 (2020).
- ⁵⁵S. Ringe, C. G. Morales-Guio, L. D. Chen, M. Fields, T. F. Jaramillo, C. Hahn, and K. Chan, "Double layer charging driven carbon dioxide adsorption limits the rate of electrochemical carbon dioxide reduction on gold," Nat. Commun. 11, 33 (2020).
- ⁵⁶S.-J. Shin, H. Choi, S. Ringe, D. H. Won, H.-S. Oh, D. H. Kim, T. Lee, D.-H. Nam, H. Kim, and C. H. Choi, "A unifying mechanism for cation effect modulating C1 and C2 productions from CO₂ electroreduction," Nat. Commun. 13, 5482 (2022).
- ⁵⁷A. Shandilya, K. Schwarz, and R. Sundararaman, "Interfacial water asymmetry at ideal electrochemical interfaces," J. Chem. Phys. **156**, 014705 (2022).
- ⁵⁸B. Tran, Y. Zhou, M. J. Janik, and S. T. Milner, "Negative dielectric constant of water at a metal interface," Phys. Rev. Lett. **131**, 248001 (2023).
- ⁵⁹R. Sundararaman and K. Schwarz, "Solvent effects determine the sign of the charges of maximum entropy and capacitance at silver electrodes," J. Chem. Phys. **158**, 121102 (2023).
- ⁶⁰S. Sarkar, A. Maitra, S. Banerjee, V. S. Thoi, and J. M. Dawlaty, "Electric fields at metal-surfactant interfaces: A combined vibrational spectroscopy and capacitance study," J. Phys. Chem. B 124, 1311–1321 (2020).
- ⁶¹M. F. Delley, E. M. Nichols, and J. M. Mayer, "Interfacial acid-base equilibria and electric fields concurrently probed by in situ surface-enhanced infrared spectroscopy," J. Am. Chem. Soc. 143, 10778–10792 (2021).
- ⁶²M. F. Delley, E. M. Nichols, and J. M. Mayer, "Electrolyte cation effects on interfacial acidity and electric fields," J. Phys. Chem. C 126, 8477–8488 (2022).
- ⁶³S. A. Sorenson, J. G. Patrow, and J. M. Dawlaty, "Solvation reaction field at the interface measured by vibrational sum frequency generation spectroscopy," J. Am. Chem. Soc. **139**, 2369– 2378 (2017).
- ⁶⁴Q. Zhu, S. K. Wallentine, G.-H. Deng, J. A. Rebstock, and L. R. Baker, "The solvation-induced onsager reaction field rather than the double-layer field controls CO₂ reduction on gold," JACS Au 2, 472–482 (2022).
- ⁶⁵S. Xue, B. Garlyyev, A. Auer, J. Kunze-Liebhäuser, and A. S. Bandarenka, "How the nature of the alkali metal cations influences the double-layer capacitance of Cu, Au, and Pt single-crystal electrodes." J. Phys. Chem. C 124, 12442–12447 (2020).
- ⁶⁶Y. Zhang, J. Tang, Z. Ni, Y. Zhao, F. Jia, Q. Luo, L. Mao, Z. Zhu, and F. Wang, "Real-time characterization of the fine structure and dynamics of an electrical double layer at electrode–electrolyte interfaces," J. Phys. Chem. Lett. 12, 5279–5285 (2021).
- ⁶⁷V. J. Ovalle, Y.-S. Hsu, N. Agrawal, M. J. Janik, and M. M. Waegele, "Correlating hydration free energy and specific adsorption of alkali metal cations during CO₂ electroreduction on Au," Nat. Catal. 5, 624–632 (2022).
- ⁶⁸J. C. Ehlers, A. A. Feidenhans'l, K. T. Therkildsen, and G. O.

- Larrazábal, "Affordable green hydrogen from alkaline water electrolysis: Key research needs from an industrial perspective," ACS Energy Lett. 8, 1502–1509 (2023).
- ⁶⁹A. Wuttig, Y. Yoon, J. Ryu, and Y. Surendranath, "Bicarbonate is not a general acid in Au-catalyzed CO₂ electroreduction," J. Am. Chem. Soc. **139**, 17109–17113 (2017).
- ⁷⁰M. C. O. Monteiro, F. Dattila, B. Hagedoorn, R. García-Muelas, N. López, and M. T. M. Koper, "Absence of CO₂ electroreduction on copper, gold and silver electrodes without metal cations in solution," Nat. Catal. 4, 654–662 (2021).
- $^{71}\mathrm{S.}$ Weng, W. L. Toh, and Y. Surendranath, "Weakly coordinating organic cations are intrinsically capable of supporting CO $_2$ reduction catalysis," J. Am. Chem. Soc. 145, 16787–16795 (2023).
- ⁷²X. Qin, T. Vegge, and H. A. Hansen, "Cation-coordinated inner-sphere CO₂ electroreduction at Au-water interfaces," J. Am. Chem. Soc. **145**, 1897–1905 (2023).
- ⁷³J. A. Rebstock, Q. Zhu, and L. R. Baker, "Comparing interfacial cation hydration at catalytic active sites and spectator sites on gold electrodes: understanding structure sensitive CO₂ reduction kinetics," Chem. Sci. 13, 7634–7643 (2022).
- ⁷⁴F. Zhang and A. C. Co, "Direct evidence of local pH change and the role of alkali cation during CO₂ electroreduction in aqueous media," Angew.Chem. Inter. Ed. **59**, 1674–1681 (2020).
- ⁷⁵A. S. Malkani, J. Anibal, and B. Xu, "Cation effect on interfacial CO₂ concentration in the electrochemical CO₂ reduction reaction," ACS Catal. **10**, 14871–14876 (2020).
- ⁷⁶M. R. Singh, Y. Kwon, Y. Lum, J. W. Ager III, and A. T. Bell, "Hydrolysis of electrolyte cations enhances the electrochemical reduction of CO₂ over Ag and Cu," J. Am. Chem. Soc. 138, 13006–13012 (2016).
- ⁷⁷O. Ayemoba and A. Cuesta, "Spectroscopic evidence of size-dependent buffering of interfacial pH by cation hydrolysis during CO₂ electroreduction," ACS Appl. Mater. Interfaces 9, 27377–27382 (2017).
- ⁷⁸S. Ringe, E. L. Clark, J. Resasco, A. Walton, B. Seger, A. T. Bell, and K. Chan, "Understanding cation effects in electrochemical CO₂ reduction," Energy Environ. Sci. **12**, 3001–3014 (2019).
- ⁷⁹G. Hussain, L. Pérez-Martínez, J.-B. Le, M. Papasizza, G. Cabello, J. Cheng, and A. Cuesta, "How cations determine the interfacial potential profile: Relevance for the CO₂ reduction reaction," Electrochim. Acta 327, 135055 (2019).
- ⁸⁰A. S. Malkani, J. Li, N. J. Oliveira, M. He, X. Chang, B. Xu, and Q. Lu, "Understanding the electric and nonelectric field compo-

- nents of the cation effect on the electrochemical CO reduction reaction," Sci. Adv. 6, eabd2569 (2020).
- ⁸¹J. N. Mills, I. T. McCrum, and M. J. Janik, "Alkali cation specific adsorption onto fcc(111) transition metal electrodes," Phys. Chem. Chem. Phys. 16, 13699–13707 (2014).
- ⁸²W. B. Jensen, "The Lewis acid-base definitions: A status report," Chem. Rev. **78**, 1–22 (1978).
- ⁸³P. C. Stair, "The concept of lewis acids and bases applied to surfaces," J. Am. Chem. Soc. **104**, 4044–4052 (1982).
- ⁸⁴L. D. Chen, M. Urushihara, K. Chan, and J. K. Nørskov, "Electric field effects in electrochemical CO₂ reduction," ACS Catal. 6, 7133–7139 (2016).
- 85D. C. Grahame, "The electrical double layer and the theory of electrocapillarity." Chem. Rev. 41, 441–501 (1947), https://doi.org/10.1021/cr60130a002.
- ⁸⁶M. T. M. Koper, "Theory of multiple proton-electron transfer reactions and its implications for electrocatalysis," Chem. Sci. 4, 2710–2723 (2013).
- ⁸⁷M. R. Singh, E. L. Clark, and A. T. Bell, "Effects of electrolyte, catalyst, and membrane composition and operating conditions on the performance of solar-driven electrochemical reduction of carbon dioxide," Phys. Chem. Chem. Phys. 17, 18924–18936 (2015).
- ⁸⁸V. J. Ovalle and M. M. Waegele, "Influence of pH and proton donor/acceptor identity on electrocatalysis in aqueous media," J. Phys. Chem. C **125**, 18567–18578 (2021).
- ⁸⁹M. C. Monteiro and M. T. Koper, "Measuring local pH in electrochemistry," Curr. Opin. Electrochem. 25, 100649 (2021).
- ⁹⁰D. S. Ripatti, T. R. Veltman, and M. W. Kanan, "Carbon monoxide gas diffusion electrolysis that produces concentrated C2 products with high single-pass conversion," Joule 3, 240–256 (2019).
- ⁹¹ J. P. Edwards, Y. Xu, C. M. Gabardo, C.-T. Dinh, J. Li, Z. Qi, A. Ozden, E. H. Sargent, and D. Sinton, "Efficient electrocatalytic conversion of carbon dioxide in a low-resistance pressurized alkaline electrolyzer," Appl. Energy 261, 114305 (2020).
- ⁹²S. S. Bhargava, E. R. Cofell, P. Chumble, D. Azmoodeh, S. Someshwar, and P. J. Kenis, "Exploring multivalent cationsbased electrolytes for CO₂ electroreduction," Electrochim. Acta 394, 139055 (2021).
- ⁹³G. A. El-Nagar, F. Haun, S. Gupta, S. Stojkovikj, and M. T. Mayer, "Unintended cation crossover influences CO₂ reduction selectivity in Cu-based zero-gap electrolysers," Nat. Commun. 14, 2062 (2023).